Letter to Editor

Dear Editor,

Thanks so much for handling our manuscript.

We write this letter to inform that based on our careful rechecks of the full computation during revision work we found that a technical bug had remained in our background climatology preparation but it in fact did not affect any main characteristics of the new method and of the conclusions we derive. The bug implied that we inadvertently had used the mean climatology of January and February of the year 2017 only, instead of the long-term mean climatology from the full range 2007 to 2017. For the revised manuscript (RM), we have hence recomputed everything based on the correct climatology and also replotted the Figures and have made needed small text adjustments.

We found that all our basic conclusions are still robust and valid; just the detailed quantifications changed, since the long-term climatology yields a somewhat different (and even more smooth) reference background. Figures 1 to 5 are very similar to the original ones. The main impact is that the threshold exceedance areas (TEAs) for the original thresholds are now somewhat smaller, while their temporal characteristics are very similar. Therefore, in the RM, we generally selected somewhat lower thresholds for calculating the TEAs and for formulating our metrics, to keep their sizes and magnitudes rather similar. The Figures 6 to 7 reflect this and confirm also that there was no qualitative change; just limited quantitative change that left the conclusions robust. Please see the RM for further details where we made small adjustments to the text accordingly and in particular also to Table 1 which concisely summarizes the chosen threshold values (which are now partly adjusted as noted above).

We note that we also explicitly added a corresponding statement and explanation to each of our two Review response documents so to make also the Reviewers clearly aware of these updates. We thank you for your understanding and hope you are also satisfied with our careful improvements.

Response to Reviewer 1 Comments

Overall comments: *This is a well-done manuscript outlining the details of and application of a novel method for detecting and evaluating sudden stratospheric warmings (SSWs). The authors aptly couch their work in the context of the ongoing discussion within the SSW community about SSW definitions. They demonstrate that their method and definitions, at leastfl for the 2009 SSW, agree with established metrics and provide additional objective information. While the context of their work is centered around the use of radio occultation data, the authors show that using a selected model's data results in complimentary analysis, showing that this work may readily be applied to long-term reanalyses. I find this work to be properly placed in the literature and a novel contribution to the community. I do have a few comments I would like the authors to address prior to publication.*

Overall Response: We thank Reviewer 1 for his/her overall positive comments. We have carefully addressed all the comments as stated below and also in the Revised Manuscript (RM).

Minor comments

Point 1: *My main concern about the manuscript is on how clear the authors are in letting the reader know that the particular threshold choices are determined based on this one anomalous event. I appreciate that they do make this clear in the conclusions section, but that clarity was missing in Section 2.3 where the threshold values are introduced. In particular, I think the paragraph beginning on page 7, line 27 could use an additional statement(s) on this topic.*

Along these lines, I think some additional clarity in the statement on pg. 12, line 1 is warranted. Certainly, this SSW is known for being strong, but as-written, the authors seem to suggest that their method is sufficient to determine that this event is strong.

Given that the work in this manuscript is based off a single SSW, it's not obvious how that can be determined independently of other SSWs.

I think the authors should critically consider other areas of the text that would benefit from further discussion about this topic.

Response 1: Thanks for these comments. Yes, we agree that it is an improvement to discuss some more details how we select our thresholds for calculating the five TEAs and for formulating the metrics. We have hence inserted more statements from lines 3 to 7 in page 8, and from lines 18 to 20 in page 8 in the RM, with text as follows:

"*As the thresholds for calculating these five TEAs, we use those defined in Table 1, (4)–(8); for example, the thresholds for MSTA are 30, 35, and 40 K as seen therein. The selection of these thresholds was mainly guided by results on the polar-mean and regional mean anomalies shown in Sections 3.1 and 3.2. We examined the temporal variations of the magnitudes of warming and cooling of the five TEAs by sensitivity checks and finally chose suitable thresholds as summarized in Table 1 for illustration*

of this 2009 event."

"*The thresholds for formulating the metrics are selected based on the condition that the TEAs calculated for the chosen thresholds can suitably capture the main features of warming or cooling of the SSW event.*"

Yes, with the statement in the first line of page 12, we should not indicate that this event is a very strong or non-so-strong one, just based on this single event. Hence we modified this from lines 14 to 16 in page 12 in the RM, as follows:

"*In lines with previous studies on this particular event, and also on recent preliminary studies on several other events, the values of main-phase duration and also of the strength indicate that this is a very strong SSW event.*"

Point 2: *The authors bring up the Butler et al. (2015) requirements for a standard definition of SSWs. Missing from the manuscript is the authors' discussion on how their definition fits these three proposed criteria. These are criteria the SSW community has agreed upon, so providing additional contextualization of their method in light of these should be done.*

Response 2: Thanks for the comments. We have added discussions from lines 8 to 15 in page 13 in the RM to state how our method meets the requirements of standard definitions of SSWs. The updated statements are as follows:

"To summarize, the metrics proposed in this study for monitoring the SSW events can well satisfy the conditions that Butler et al. (2015) suggest for proposing a standard definition (cf. Section 1). Firstly, our approach well captures the sudden warming of the main phase and also its downward propagation into the lower stratosphere as well as the cooling occurring after the warming phase in the upper stratosphere. Secondly, the approach can be used for both RO and other suitable profile data and likewise for reanalysis data, and can be applied for both post-processing and in real time. Finally, the new approach is using anomalies over several height layers, and TEAs over larger area, and hence the detection and monitoring results are not sensitive to details such as exact latitude or pressure level. Potential further refinements of the thresholds for our metrics will be determined from recently started work on multiple SSW events, using longer-term data over the recent decades."

Specific comments

Point 1: *Do the authors report somewhere that bending angle and density are given in normalized units? This is apparent, but the reader would benefit from a definitive statement in the manuscript. As well, please state how the normalization is performed (normalized with respect to what?).*

Response 1: We have in fact shown the equations of how to calculate anomalies from (1) to (3) in our Table 1, which is used to concisely summarize our methodology of the full approach. To make this clearer, we have added the following statements from lines 20 to 22 in page 6 in the RM:

"*Temperature anomalies are calculated as absolute values, while density and bending angle anomalies are calculated as relative (percentage) values, by dividing the absolute-value anomaly profiles by the collocated climatological profiles.*"

Point 2: *Abstract, line 20: recommend "has strong potential."*
Response 2: Thanks, we have corrected to "has strong potential" in the RM.

Point 3: *Abstract, lines 17 and 22: is it necessary to introduce these metrics – the 3 Mio. km^2 threshold and the MSTA-TEA40 metric – here? I'm not sure that the abstract benefits from either the specificity of the former or the raising of the as-yet undefined metric and abbreviation of the latter. I would recommend removal unless the authors have strong objections.*
Response 3: Thanks for this suggestion. In the RM, we have avoided to introduce the metrics in the abstract. We improved the sentence from lines 22 to 23 in the first page in the RM as follows:

"temperature anomalies over the middle stratosphere exceeding 35 K cover an area more than 10 Mio. km^2."

Point 4: *Pg. 8, lines 25-26: I'm not quite sure I follow what's being said here. Is it that the specific definitions the authors have proposed may change as more systematic study is performed?*
Response 4: Yes, we try to say that the we can tell whether the SSW event is a strong one or a more minor one from our recorded duration and also strength. However, we agree that we can only know the specific values or thresholds of such determination of SSW events by applying our method to longer-term data records. By then, we can more robustly propose a definition for SSW based on the determination thresholds. To make our statements clearer for now in this initial introduction of the method, we have corrected the corresponding sentences from lines 5 to 6 in page 9 in the RM as follows:

"*However, the specific thresholds for our metrics and indicators for SSW detection, monitoring, and classification can only be determined after the new approach is applied to longer-term data containing multiple events.*"

We thank Reviewer 1 for his/her comments again. In addition to the comments and suggestions from the Reviewers, we inform that based on our careful rechecks of the full computation we found that a technical bug remained in our original calculation of the background climatology. It implied that we inadvertently had used the mean climatology of January and February of the year 2017 only, instead of the long-term mean climatology from the full range 2007 to 2017. We have corrected this in the updated RM.
We found that all our basic conclusions are still robust and valid; just the detailed quantifications changed, since the long-term climatology yields a somewhat different (and even more smooth) reference background. Figures 1 to 5 are very similar to the

original ones. The main impact is that the TEAs from the original thresholds are now smaller, while the TEAs temporal characteristics are strongly similar. Therefore, in the RM, we generally selected somewhat lower thresholds for calculating TEAs and for formulating our metrics, to keep their sizes and magnitudes rather similar. The Figures 6 to 7 reflect this and confirm that there was no qualitative change, just limited quantitative change that left the conclusions robust. Please find the RM for further details where we made small adjustments to the text accordingly.

Response to Reviewer 3 Comments

General comments: *This paper proposes a new application of GNSS-RO for detecting stratospheric sudden warming (SSW) events. I appreciate the devoted efforts of the authors for developing an interesting analysis technique with the COSMIC GNSS-RO data and applying it to the major SSW event that occurred in 2009. The results are impressive in visualizing the horizontal distribution as well as the time evolution of the 2009 SSW event. However, I have several concerns about the data analysis procedure and the usefulness of the proposed techniques.*

Overall response: We thank Reviewer 3 for his/her comments. We have carefully addressed all the comments as stated below and also in the Revised Manuscript (RM).

Major comments:

Point 1: *This method is successfully applied to the SSW event of January 2009, which is a well-studied case. I am afraid that Section 3 is too descriptive. For comparing the analyzed results with earlier studies, any new scientific findings on SSW behavior should be reported. The technique should be evaluated, showing any new features of the SSW that can be uniquely resolved by GNSS-RO data.*

Response 1: Thanks for the comments. As we have discussed in the introduction section of this paper, one key motivation of this initial paper is to pave the way towards an improved standard definition of SSW, and such a definition does not exist yet due to lack of sufficiently reliable observational data and also the diversity of application purposes. Therefore, we intend to propose a robust method to detect SSW and subsequently to propose a standard definition of SSWs.

For our initial study here, we used this typical 2009 SSW event. The new method shows its basic potential for reliable SSW detection. The results obtained using this new method are consistent with results shown by previous researches. We will apply this new method in future to longer-term data records, and have just very recently started this work, to refine our specific settings and also thresholds to finally make a broadly useful SSW detection method. Based on this we also intend to introduce a standard definition of SSWs.

The prime new features of this study are hence in our method design. It can satisfy the requirements that were outlined by Butler et al. (2015), reading as follows (cited from line 33 to 34 in page 3 and from lines 1 to 2 in page 4 in the RM):

"*The new definition should be proposed primarily for the purpose of describing polar winter variability. Secondly, it should be easily calculated and applicable to reanalysis and model outputs, both in post-processing and in real time. Finally, the new definition should not be highly sensitive to details, such as an exact latitude, background climatology, threshold wind speed, spatial extent, or pressure level.*"

Our proposed method can describe the variability over all polar region before, during

and after the occurrence of SSWs and also over different stratospheric layers. The new features of our new method include that:

(1) It can be applied to RO and similar profile data, and also gridded reanalysis data such as from ECMWF.

(2) It uses anomalies over selected height layers and also introduces the concept of TEAs, robustly quantifying warming or cooling areas in polar region. This design makes our method properly insensitive to any perturbing fine details.

(3) RO bending angles, and density profiles, are found useful auxiliary variables for SSW detection, but it similarly works for temperature-only data as well.

Based on our new method, Section 3 also shows all new findings obtained using our new method, including our metrics, TEAs and also RO bending angles anomalies during SSW, which have not been analyzed by any other previous researchers.

To make our new features clearer for readers to comprehend, as also suggested by Reviewer 1, we have added some discussions at the end of Section 3 (from lines 8 to 15 in page 13 in the RM), as follows:

"To summarize, the metrics proposed in this study for monitoring the SSW events can well satisfy the conditions that Butler et al. (2015) suggest for proposing a standard definition (cf. Section 1). Firstly, our approach well captures the sudden warming of the main phase and also its downward propagation into the lower stratosphere as well as the cooling occurring after the warming phase in the upper stratosphere. Secondly, the approach can be used for both RO and other suitable profile data and likewise for reanalysis data, and can be applied for both post-processing and in real time. Finally, the new approach is using anomalies over several height layers, and TEAs over larger area, and hence the detection and monitoring results are not sensitive to details such as exact latitude or pressure level. Potential further refinements of the thresholds for our metrics will be determined from recently started work on multiple SSW events, using longer-term data over the recent decades."

Point 2: *Before proposing this method to monitor major/minor SSW events from long-term records, more cases should be tested to confirm that it is fully robust.*
Response 2: Thanks for this comment. Yes, we will make sure this method is fully robust by applying this method to nearly 1.5 decades (14 years) of RO data and also several decades of ERA-5 data, as we stated in the original manuscript (and see now lines 16 to 18 in page 14 in the RM, where we updated that the winter half year 2019/20 is now as well already available):

"*Based on the encouraging demonstration in this study, follow-on work will apply the method to long-term RO and reanalysis datasets (RO overlapping 2006–2020 with reanalyses over 1979–2020) and assess its utility for long-term SSW monitoring.*"

Point 3: *SSW is defined by the temperature anomaly in this study, but it is also characterized by zonal wind reversal. As GNSS-RO can provide only the former*

information, it may not clarify the entire behavior of SSW; therefore, this method may not be considered as primary. (See comment 1.)

Response 3: Thanks for the comment. As what has been discussed by Butler et al. (2015, 2018) and also in this paper, there is currently no standard definition of SSWs. There are currently nine often used definitions, in terms of zonal-mean winds at 10 hPa and 60° latitude, geopotential height anomalies, and also temperature anomalies, etc. Among these definitions, SSWs characterized by zonal wind reversal is one of the common used definitions. However, this does not mean that SSW definitions must be characterized by wind reversals.

According to literature, the SSW phenomena was first noted by its sudden and quick temperature increase measured by radiosonde since the 1950s. Wind reversal is one of its important characteristics occurring during this sudden warming. It is a useful metric for SSW. However, we also noted that selection of certain altitude and also latitude for measuring of wind reversals can results in different detection results. The SSW climatology obtained from previous studies, by using wind reversals at 65°N and 60°N, could result in very different results in some cases, with the center day varying more than 2 weeks. From this, we can see that if characterizing SSWs by wind reversals, results may suffer from detailed selection of latitudes.

Our method, which is relying on anomalies over several selected altitude layers, and also large threshold exceedance areas (TEAs), is not sensitive to such detail selection. The method is also not only suitable for RO or similar profile data, and also allows for real-time applications, and can likewise be applied to reanalysis data. Since reanalysis data also provide wind information, users who prefer to use reanalysis data could also extract wind information together with our method for SSW detection.

For our treatment in the manuscript, we tried to indeed provide an informative introduction and overview of this (without excessive length); and please see also our response to comment 1.

Point 4: *The analysis procedure is a bit complicated. It employs three anomaly parameters: temperature, density, and bending angle, in four altitude ranges. Out of a total of 12 values, only five parameters listed in Table 1 are used to monitor the SSW characteristics. It is not clear whether the selection of these five parameters will generally be adopted for any SSW event, or this set is used specifically for the 2009 SSW event.*

Response 4: Thanks for the comment. For formulating our metrics, we select five TEAs based on five thresholds. These thresholds will be further refined after we apply our method to longer data records, a work we just recently started. The method will then can be adopted for any SSW event.

Point 5: *Assuming that the COSMIC GNSS-RO data is assimilated into ECMWF, the 2009 SSW naturally appears similar in both GNSS-RO and ECMWF. Therefore, agreement of the SSW characteristics, as shown in Fig. 4, does not necessarily*

confirm the validity of the proposed GNSS-RO method.

Response 5: Thanks for the comments. The proposed method does in fact not just rely on RO data. As noted in a response above already, it is a method that can use both RO data and/or analysis data from model, such as ECMWF data. If other observation data can offer global dense distributed and high quality atmospheric profiling data over the stratosphere, the data can also be applied to this method.

The reason we incorporate RO data, but not just the model data is because RO data can provide accurate profiling for climate-type monitoring, but also available in form of real-time observation of the atmosphere. Furthermore, RO data have several distinctive advantages, such as the high vertical resolution in stratosphere (~1 km), global coverage with very repeatable quality, and the availability of useful auxiliary variables such as RO bending angles. It is such advantages that make RO data quite suitable for SSW detection on their own.

The impacts of assimilation of RO data into ECMWF is that ECMWF analysis data have higher accuracy in regions, where RO data of high density and accuracy that other observation data. It does not affect the validity of our method to ECMWF data at all.

Point 6: *The accuracy of the GNSS-RO data in the upper stratosphere and mesosphere (above about 40–50 km) should be tested carefully, because the error in the bending angle due to ionospheric effects could dominate, depending on the ionospheric conditions. Moreover, it is noteworthy that the bending angle profile at high altitudes is heavily optimized by referring to a model atmosphere profile, reducing the deviations from a climatological profile.*

Response 6: In our original manuscript, though we used so-called optimized bending angle, we have internally tested that using the ionosphere-corrected atmospheric bending angles directly (i.e., non-optimized bending angles) are very similar to the results from using optimized bending angle. In order to avoid this confusion in our revised manuscript, we only used the atmospheric bending angles for the calculation of bending angle anomalies now, so that "optimization" cannot play any role. In this form, atmospheric bending angles are indeed independent observations not affected by background model atmospheric profiles. In order to avoid somewhat higher short-scale variability of these non-optimized bending angles, we use a 2 km vertical averaging for smoothing over the short-scale variations. We tested again, and found confirmed, that the results from using the atmospheric bending angles directly are similar to the ones using optimized bending angles. The RM includes these updates accordingly. The figures related to bending angle are all updated to use non-optimized bending angle. We have also used describe this in the text from lines 22 to 23 in page 6 as below:

"*In order to avoid the impacts of background model on bending angles, we used non-optimized bending angle in our study.*"

Point 7: *As the analyzed values are a weighted mean over three days, the time resolution is longer than one day. Therefore, the time evolution of the SSW event,*

such as its duration and onset date, cannot be precisely determined at a daily resolution.

Response 7: What we do (as we describe) is that we use a weighted mean over three days, just to allow more RO events for a reliable statistical calculation. However, in order to get our daily sampling to achieve a near-daily resolution, we give the data of the middle day a twice-high weight of 0.5, while the weights of the predecessor and successor days are only 0.25. In this way the daily sampling is indeed still meaningful, while we statistically improve the robustness of the average profiles from enabling a bigger ensemble of profiles for the weighted averaging, by taking 3-day windows.

We note also that we have made detail sensitivity tests to make sure that our selection of temporal resolution is robust. We have calculated anomalies by just using one day's data and we have also calculated anomalies by using same weight of all three days (each day 1/3), etc. We found that if just using one day's data, the magnitudes of the resulting anomalies are similar to our weighted mean over three days, but somewhat nosier. If using three days' mean with even weights for all days, the dynamic daily evaluation of SSWs would be somewhat more blurred. So at the end we chose, as a most suitable trade-off, the weighted averaging that favors the center day's weight as noted above.

In order to make this clearer also for readers, we have added the following statements from lines 16 to 19 in page 7 as below:

"*In this way the daily sampling is indeed still meaningful, while we statistically improve the robustness of the average profiles from enabling a bigger ensemble of profiles for the weighted averaging, by taking 3-day windows.*"

Point 8: *I would encourage the authors to extend the latitude range below 60_N, as the effects of SSW on the middle latitudes and equatorial regions have been the subject of recent research. I would also suggest the use of ionospheric electron density data with GNSS-RO to identify SSW effects on the upper atmosphere.*

Response 8: Thanks for the comment. However, in this initial paper we prefer not to study at the same time the effects of SSWs on the middle latitudes and equatorial regions, but rather focus on introducing a robust new SSW detection method. Therefore, we decided on this focus on polar region here, though in future we are indeed interested to analyze also "teleconnection effects" towards the lower latitudes. Similarly, using of ionospheric electron density data to identify SSW effects are also beyond the focus in this study.

Specific comments:

Point 9: P2, L27–30: Show some references on the limitations of other satellite missions.

Response 9: OK. We have added two new references, i.e., McInturff, et al. (1978) and

Manney et al. (2008), which have discussed the limitations of conventional satellites data. Please refer to line 29 amd 30 in page 2 in the RM.

Point 10: *P3, L1–3: Similarly, explain the limitations of the reanalysis data, referring to the relevant papers.*
Response 10: OK. We have added the Butler et al. (2015) also as a reference here, which have discussed the limitations of the reanalysis data. Please refer to line 3 in page 3 in the RM.

Point 11: *P5, L19–25: GNSS-RO data are neither distributed evenly nor regularly, but randomly with a relatively high horizontal density.*
Response 11: Thanks, yes. In order to make this description more accurate, we have updated the corresponding statements from lines 20 to 24 in page 5, now stated as follows:

"*The upper panel shows the distribution of RO observations in the study domain from 50° N to North Pole, within which strong warmings were found by previous studies of the SSW event (Labitzke and Kunze, 2009; Harada et al., 2010; Kodera et al., 2011; Taguchi et al., 2011). It can be seen that most of the polar region is covered by RO observations. Similarly, high observation density also applies to the other days of the study period."*

Point 12: P6, L23–25: Is the GNSS-RO data assimilated into the ECMWF? If so, the agreement of the climatology is reasonable. (See comment 5.)
Response 12: Thanks, yes. And as responded to Point 5, assimilation of GNSS-RO data does not affect the application of our method, which can be applied to both RO and ECMWF data.

Point 13: P6, L32: Remove one of "the".
Response 13: Thanks. We have deleted this "the" in the RM.

Point 14: P7, L9–11: Temporal resolution is lower than one day, which affects the description of the time evolution of SSW, such as its duration and onset date. (See comment 7.)
Response 14: Thanks. Following up to our response to Point 7 above, our strategy of three days' averaging by given the center day twice the weight does not appreciably affect the quantification of the time evolution of SSWs, based on our sensitivity tests. We have also applied our method to the regularly sampled ECMWF data (2.5*2.5 grid points and four time layers a day), without such three days' averaging for these data, but the conclusions are still the same as the other results discussed.

Point 15: P7, L14–17: For the four altitude regions, the exact height ranges should be provided here, even though they are shown in Table 1.
Response 15: Thanks. We have added the corresponding altitude ranges we used for these five TEAs (in lines 31 to 32 in page 7 in the RM).

Point 16. P7, L30–34: Is selection of the thresholds intended to be applicable to any SSW events, or specific to the 2009 case? (See comment 4.)

Response 16: These thresholds are currently applied to this 2009 case. We will refine these thresholds after we have applied our method to longer-term data records, which is a work just recently started. However, the method will be the same as now, but only with some refined threshold definitions.

We have discussed this in the original manuscript and now further updated the corresponding discussion (in lines 3 to 6 in page 9, in the RM and in lines 16 to 23 in page 14 in the conclusion part of the RM), as follows:

"In a follow-on work using long-term RO and reanalysis datasets, these indicators will be used to detect SSW events, for example by requiring a minimum main-phase duration of 7 days or so to qualify as an SSW, and to record the strength of the events. However, the specific thresholds for our metrics and indicators for SSW detection, monitoring, and classification can only be determined after the new approach is applied to longer-term data containing multiple events."

"*Based on the encouraging demonstration in this study, follow-on work will apply the method to long-term RO and reanalysis datasets (RO overlapping 2006–2020 with reanalyses over 1979–2020) and assess its utility for long-term SSW monitoring. In this way, the most suitable settings to use for the duration, area, and overall strengths indicators for robust SSW detection, monitoring, and classification can be determined.*

In addition, we will be able to learn how the possible advantages in long-term stability and accuracy of the RO data play out or not in SSW monitoring in comparison to reanalysis data, including for different variants of RO processing and reanalysis. Overall, we expect the approach to be valuable for monitoring how SSW characteristics unfold event by event but also, and in particular, how they possibly vary under transient climate change and how they tele-connect to lower latitude regions."

Point 17. P8, L2: Isn't 50% of the density deviation reasonable? It seems too large. (See comment 6.)

Response 17: Thanks for the comments. We have double checked all data and computations and find the density anomaly magnitudes up to roughly these levels, which are also consistent with bending angle anomaly sizes. Since many existing studies show polar mean anomalies or anomalies smoothed over multi-day periods, the anomaly magnitudes are somewhat smaller with those stronger smoothings. Here we exploit regional mean anomalies which are based on relatively small bin areas (5°×20°) on a daily sampling basis, therefore, the magnitudes are somewhat larger. See also the comment appended at the end of this response document; a technical correction (using the correct long-term background climatology) also made the anomalies a bit smaller, though in general for strong SSW events like this one in 2009 they reach these magnitudes.

Point 18. P8, L13: The word “then” can be read as “than”, right?
Response 18: Yes, thanks for pointing this out. We have corrected “then” to “than” in the RM (line 23 in page 8 in the RM).

Point 19. P8, L19–20: “number of days”. (See comment 14.)
Response 19: The “number of days” here suggests the number of days that our main-phase records last. Regarding the concern about the daily temporal resolution, please see our response to Points 7 and 14 above.

Point 20. P8, L22–23: How is the technique adjusted for long-term data? It sounds like this method is not fully robust, and a specific tuning is required for each SSW event. (See comment 4.)
Response 20: We have not applied this method to longer-term data in this initial study, we just very recently started such work. From our researches on this 2009 event, and also some complementary cross-check analyses (on the polar-cap mean, on daily mean anomalies of other years, etc.) we found that our selection of thresholds is basically reasonable. Yet, as mentioned already above in our response to Point 2, in follow-on work we will apply our method to almost 1.5 decades (14 years) of RO data and several decades of ERA-5 data, to refine our specific thresholds and make our method fully robust for the detection of multiple SSW events of various strengths.

Point 21. P9, L26–28: "differences above 50 km". (See comment 6.)
Response 21: Please refer to our Response to Point 6.

Point 22. Section 3, P11, L24–26: I encourage the authors to show any new scientific findings obtained with the GNSS-RO data. (See comments 1 and 3.)
Response 22: Please see our extended response to Points 1 and 3. The method itself is all new so we prefer to keep the length and scope of this manuscript in its current form. We will be interested in such extended scopes in follow-on work. As to the new content of this manuscript, we note that Section 2 and also the results in Section 3 are all essentially new developments and findings of this paper.

We thank Reviewer 3 for his/her comments again. In addition to the comments and suggestions from the Reviewers, we inform that based on our careful rechecks of the full computation we found that a technical bug remained in our original calculation of the background climatology. It implied that we inadvertently had used the mean climatology of January and February of the year 2017 only, instead of the long-term mean climatology from the full range 2007 to 2017. We have corrected this in the updated RM.
We found that all our basic conclusions are still robust and valid; just the detailed quantifications changed, since the long-term climatology yields a somewhat different (and even more smooth) reference background. Figures 1 to 5 are very similar to the original ones. The main impact is that the TEAs from the original thresholds are now

smaller, while the TEAs temporal characteristics are strongly similar. Therefore, in the RM, we generally selected somewhat lower thresholds for calculating TEAs and for formulating our metrics, to keep their sizes and magnitudes rather similar. The Figures 6 to 7 reflect this and confirm that there was no qualitative change, just limited quantitative change that left the conclusions robust. Please find the RM for further details where we made small adjustments to the text accordingly.

Monitoring Sudden Stratospheric Warmings using radio occultation: a new approach demonstrated based on the 2009 event

Ying Li[1], Gottfried Kirchengast[2], Marc Schwärz[2], Florian Ladstädter[2], Yunbin Yuan[1]

[1] State Key Laboratory of Geodesy and Earth's Dynamics, Innovation Academy for Precision Measurement Science and Technology (APM), Chinese Academy of Sciences, Wuhan, 430071, China
[2] Wegener Center for Climate and Global Change (WEGC) and Institute for Geophysics, Astrophysics, and Meteorology/ Institute of Physics, University of Graz, 8010 Graz, Austria

Correspondence to: Ying Li (liying@asch.whigg.ac.cn)

Abstract. We introduce a new method to detect and monitor Sudden Stratospheric Warming (SSW) events using Global Navigation Satellite System (GNSS) Radio Occultation (RO) data at high northern latitudes and demonstrate it for the well-known Jan-Feb 2009 event. We first construct RO temperature, density, and bending angle anomaly profiles and estimate vertical-mean anomalies in selected altitude layers. These mean anomalies are then averaged into a daily-updated 5 ° latitude × 20 ° longitude grid over 50 ºN – 90 ºN. Based on the gridded mean anomalies, we employ the concept of Threshold Exceedance Areas (TEAs), the geographic areas wherein the anomalies exceed predefined threshold values such as 35 K or 35 %. We estimate five basic TEAs for selected altitude layers and thresholds and use them to derive primary-, secondary-, and trailing-phase TEA metrics to detect SSWs and to monitor in particular their main-phase (primary- plus secondary-phase) evolution on a daily basis. As an initial setting, the main-phase requires daily TEAs to exceed 3 Mio. km^2, based on which main-phase duration, area, and overall event strength are recorded. Using the Jan-Feb 2009 SSW event for demonstration, and employing RO data plus cross-evaluation data from analysis fields of the European Centre for Medium-range Weather Forecasts (ECMWF), we find the new approach has strong potential for detecting and monitoring SSW events. The TEA metrics show a strong SSW emerging on Jan 18, reaching a maximum on Jan 22, and the strong primary-phase temperature anomaly fading by Jan 26. On Jan 22–23, temperature anomalies over the middle stratosphere exceeding 35 K cover an area of more than 10 Mio. km^2. The geographic tracking of the SSW showed that it was centered over East Greenland, covering Greenland entirely and extending from Western Norway to the west of Greenland. The secondary- and trailing-phase metrics track the further SSW development, where the thermodynamic anomaly propagated downward and was fading with a transient upper stratospheric cooling, spanning until end February and beyond. Given the encouraging demonstration results, we expect the method very suitable for long-term monitoring of how SSW characteristics evolve under climate change and variability using both RO and reanalysis data.

删除的内容:
删除的内容: 40
删除的内容: 40
删除的内容: of
删除的内容: 17
删除的内容: 23
删除的内容: 27
删除的内容: a MSTA-TEA40 value (TEA of
删除的内容: temperature anomaly >40
删除的内容:)
删除的内容: about 9
删除的内容:
删除的内容: was reached
删除的内容: Eastern Canada.

1 Introduction

Sudden Stratospheric Warming events (SSWs) are strong and highly dynamic phenomena that often occur in the northern polar stratosphere (McInturff et al., 1978; Butler et al., 2015, Butler et al., 2018). Such events are characterized by a rapid increase of temperature (> 30 to 40 K) in the middle and upper stratosphere accompanied by vortex displacements or even splits (Charlton and Polvani, 2007). Occurrence of SSWs is generally believed to be caused by tropospheric planetary waves which penetrate into the stratosphere, mediated by the Quasi-Biennial Oscillation (QBO) and the Southern Oscillation (SO) in the tropics (Thompson et al., 2002; Labitzke and Kunze, 2009). Such waves influence the stratospheric polar vortex and cause a warming in the upper stratosphere and mesosphere.

The warming will propagate gradually downward and cause an anomalous widespread warming that persists for several weeks (Baldwin and Dunkerton, 2001; Hitchcock and Shepherd, 2013; Dhaka et al., 2015; Newman et al., 2018). Following the initial warming, a cold anomaly forms in the upper stratosphere that also causes an elevated stratopause (Siskind et al., 2007; Manney et al., 2008; Hitchcock and Shepherd, 2013). The tropical atmosphere is as well found to be influenced (Kodera et al., 2011; Yoshida and Yamazaki, 2011; Dhaka et al., 2015). Cooling can be observed in the tropical stratosphere and also the tropopause is found altered (Yoshida and Yamazaki, 2011; Dhaka et al., 2015). Furthermore, gravity wave activity, cirrus cloud formation and electron density of ionosphere are all found affected by SSWs (Eguchi, N., Kodera, K. 2010; Yue et al., 2010; Sathishkumar and Sridharan, 2011; Kohma and Sato, 2014). Due to such strong impacts and far-reaching teleconnections of SSWs, it is hence important to detect and monitor SSW events in a robust and reliable way.

The observation and detection of SSWs requires evenly distributed and accurate height-resolved observations of the stratosphere at high latitudes. However, robust techniques providing high-quality observations in these remote regions are notoriously sparse. Past researches mainly used radiosonde, rocketsonde, conventional satellite or reanalysis data to study SSWs (McInturff et al., 1978; Charlton and Polvani, 2007; Manney et al., 2008, 2009; Hitchcock and Shepherd, 2013). However, both radiosonde and rocketsonde cannot provide evenly-distributed observations due to their mostly land-limited properties. Furthermore, since vulnerable to radiation biases and constrained by elevation limits, few radiosondes can provide data above 30 km (Butler et al., 2015).

With the advent of the satellite era, it became possible to put passive sounding instruments, such as microwave limb sounders and infrared radiometers, on satellites to observe the atmosphere (e.g., Charlton et al., 2007; Manney et al., 2008, Manney et al., 2009). Due to the movements of the satellites, observations are globally distributed, in principle. However, satellite passive sounding data come in the form of radiances and no unique solution then exists, in terms of the radiative transfer equation, to accurately convert radiances to height-resolved temperature or winds, which are key variables for SSW monitoring (McInturff, et al., 1978, Manney et al., 2008). Therefore, the fit-for-purpose of measurements from these instruments is limited.

With the development of atmospheric data assimilation systems, re-analysis data have become a quite reliable data source for long-term atmospheric analysis, due to their advantages of regularly distributed data in space and time and their capability to provide data up into the mesosphere (Charlton et al., 2007; Yoshida and Yamazaki, 2011; Butler et al., 2018). However, re-

删除的内容: evenly

删除的内容: .

analysis data may have inhomogeneities and irregularities in the long-term, due to observation system updates and varying analysis biases in sparsely observed domains, which may limit their long-term stability in monitoring SSWs and possible changes in their characteristics due to climate change and interannual variability (Butler et al., 2015).

As a consequence of the limitations of classical observations and re-analyses data, there is currently no standard definition of SSWs. Early definitions were usually based on temperature increases and wind reversals. An often used early definition was provided by McInturff in 1978, presented in one of the reports of World Meteorological Organization (WMO) Commission for Atmospheric Sciences (CAS): 1. A stratospheric warming can be called minor if a significant temperature increase is observed of at least 25 °degrees in a week or less at any stratospheric level in any area of the wintertime hemisphere and if criteria for major warmings are not met; 2. A stratospheric warming can be said to be major if at 10 mb or below the latitudinal mean temperature increase poleward from 60 °degrees and an associated circulation reversal is observed. This definition has been dominated over the 1980s and 1990s though the detailed interpretations could be different, e.g., using observations below 10 mb, or using wind observations at 65 ºN degrees, etc.

With the development of observation techniques, several new definitions for characterizing SSWs have been proposed. Butler et al., 2015 made a detailed literature review on the definitions of SSW and discussed as many as 9 often used definitions of SSWs, such as zonal-mean zonal winds at 10 hPa and 60 °latitude (Christiansen 2001; Charlton and Polvani, 2007), polar cap-averaged geopotential height anomalies at 10 hPa (e.g., Thompson et al., 2002), Empirical Orthogonal Functions (EOFs) of gridded pressure-level data of geopotential height anomalies (Baldwin and Dunkerton 2001; Baldwin 2001), zonal wind anomalies (Limpasuvan et al. 2004) or temperature anomalies (e.g., Kuroda and Kodera 2004; Hitchcock and Shepherd 2013; Hitchcock et al., 2013). Each definition has unique characteristics and application purposes, e.g., EOFs of height anomalies focus more on the stratosphere-troposphere coupling.

One of the most commonly used SSW definitions in recent studies is the one based on zonal-mean zonal wind at 60 ºN. This definition has been used in several previous studies though interpretation could be slightly different (e.g., Andrews et al., 1985; Labitzke and Naujokat 2000) and was described in detail by Charlton and Polvani, 2007 (denoted as CP07 below). According to the CP07 definition, a major midwinter warming occurs when the zonal mean zonal winds at 60 ºN and 10 hPa become easterly during winter, defined here as (November-March (NDJFM)). The first day on which the daily mean zonal mean zonal wind at 60 ºN and 10 hPa becomes easterly is defined as the central date of the warming. Once SSW events have been identified, they are classified into polar vortex displacements or split ones by identifying the number and relative sizes of cyclonic vortices during the evolution of the warming.

From the above, we can find that it would be impossible to find a single definition to serve every purpose to describe every event perfectly. However, it is still important to find a standard definition for the purposes of statistical assessments, based on historical data and future climate simulations. Butler et al. (2015) suggest that with the development of observation techniques, it is time again to propose a standard definition of SSWs. The new definition should be proposed primarily for the purpose of describing polar winter variability. Secondly, it should be easily calculated and applicable to reanalysis and model outputs,

删除的内容: .

both in post-processing and in real time. Finally, the new definition should not be highly sensitive to details, such as an exact latitude, background climatology, threshold wind speed, spatial extent, or pressure level.

Since the early 2000s, Global Navigation Satellite System (GNSS) radio occultation (RO) has become a new and reliable data source for weather and climate studies (e.g., Kursinski et al., 1997; Steiner et al., 2001; Hajj et al., 2002; Anthes, 2011; Steiner et al., 2011). The RO technique uses GNSS receiver instruments on low Earth orbit satellites to receive GNSS signals for active atmospheric limb sounding in occultation geometry. As the signals propagate through the atmosphere, they are phase-delayed and bent in their path, due to vertical refractivity gradients determined by density and temperature changes. Building on these properties, accurate bending angle profiles can be retrieved from RO signal phase delays, which are highly stable during the measurement time of vertically scanning from mesopause into the troposphere (setting events) or from troposphere into mesopause (rising events) of just about one minute, called an RO event. The bending angle profile is then converted to a refractivity profile (via an Abel transform), which is directly proportional to the density profile in the stratosphere (refractivity equation), from which then the pressure profile (via hydrostatic integration) and finally temperature profile (via equation of state) is derived.

The vertical resolution of RO in the stratosphere is about 1 km, supporting height-resolved studies, and validation results against radiosonde and (re-)analysis data suggest that RO data are of small discrepancy to these in the upper troposphere and lower stratosphere (Scherllin-Pirscher et al., 2011a; 2011b; Ladstädter et al., 2015). Finally, RO data can be combined without the need of inter-calibration, which makes them very suitable for climate-related studies (Foelsche et al. 2011; Steiner et al., 2011; 2013; 2020). Due to these distinctive advantages, RO data have been successfully used in many weather and climate studies and are hence a promising data source also for detecting and monitoring SSWs. Since continuous multi-satellite RO data started in 2006 (see Sect. 2 below), the geographic data coverage is sufficiently dense for monitoring and analyzing regional-scale phenomena such as SSWs. Complementary to reanalysis datasets, which also offer dense coverage, RO reprocessing datasets hence feature an accurate and long-term stable observational data record of climate benchmark quality (Steiner et al., 2020), allowing stable conditions for SSW monitoring over decades. Therefore, given the high complementarity of these observations to reanalysis (Bosilovich et al., 2013; Parker, 2016; Simmons et al., 2020), RO data well fulfill the requirements presented by Butler et al. (2015).

A couple of studies have used RO data to analyze SSW already. For example, Wang et al. (2009) have used RO to study SSW influences on gravity waves during events in 2007-2008. Yue et al. (2010) and Lin et al. (2012) have used RO data to study ionospheric variations related to the 2009 SSW event. Klingler (2014) has used RO data to examine the temperature changes during the 2009 SSW event, and compared the results to European Centre for Medium-Range Weather Forecasts (ECMWF) data, while Dhaka et al. (2015) have used them to study the dynamical coupling between polar and tropical regions during this event.

In this study, we use RO data to introduce a new method to detect and monitor SSW events. As a demonstration case, the Jan-Feb 2009 SSW event was used, since this is well known from other studies (such as the ones just cited above) and therefore context knowledge is good. As a cross-check and for evaluation of robustness, ECMWF analysis data are also used and the

results are compared to those with RO data. The paper is arranged as follows. Section 2 introduces the data and methodology. Section 3 introduces the detection and monitoring results. Section 4 provides our conclusions.

2 Data and methodology

2.1 Radio occultation data

Continuous RO data started in 2001 with the Challenging Mini-satellite Payload mission (CHAMP; Wickert et al., 2001), followed by the Gravity Recovery and Climate Experiment (GRACE; Wickert et al., 2005), the Constellation Observing System for Meteorology, Ionosphere and Climate (COSMIC; Schreiner et al., 2007), the European Meteorological Operational satellites (MetOp; Luntama et al., 2008), the Chinese FengYun-3C operational satellite (Sun et al., 2018), and others. These missions, especially the launch of the COSMIC mission in 2006, which was a constellation of six satellites, have ensured as of 2006 a sufficient coverage with RO event observations for regional-scale studies such as of SSWs.

In this study, we use the atmospheric RO profile data from the Wegener Center for Climate and Global Change (WEGC), processed by its latest Occultation Processing System version 5.6 (denoted as OPSv5.6 hereafter). Several studies that introduced, validated and evaluated these OPSv5.6 data (e.g., Ladstädter et al., 2015; Schwärz et al., 2016; Angerer et al., 2017; Scherllin-Pirscher et al., 2017) as well as inter-comparison to other RO center datasets (Steiner et al., 2020) show that the OPSv5.6 stratospheric profiling data of interest in this study are of high quality for the purpose. For a detailed discussion of quality aspects of the OPSv5.6 data we refer to Angerer et al. (2017). We use the high quality-flagged temperature, density, and bending angle profiles over Jan-Feb 2009, the time period of our demonstration study, in the northern high latitude study domain of 50–90 °N.

Figure 1 illustrates the distribution of RO events on 23 Jan 2009 and the number of RO events we used per day over Jan–Feb 2009. The upper panel shows the distribution of RO observations in the study domain from 50 °N to North Pole, within which strong warmings were found by previous studies of the SSW event (Labitzke and Kunze, 2009; Harada et al., 2010; Kodera et al., 2011; Taguchi et al., 2011). It can be seen that most of the polar region is covered by RO observations. Similarly, high observation density also applies to the other days of the study period. The bottom panel shows that daily numbers of RO events within the three successively smaller polar cap regions 50 °– 90 °N, 60 °– 90 °N, and 70 °– 90 °N are within about 500–700, 300–400, and 150–200 RO events per day, respectively. This is typical for the RO observation period as of 2006 and sufficiently dense for robust SSW monitoring as we will see.

2.2 ECMWF analysis data

As mentioned in Sect. 1, a robust SSW definition should not only be applied to observation data, but also be readily applicable to (re)analysis and model outputs with their regular-gridded datasets. Therefore, we also use operational analysis data from the ECMWF over the same study period for cross-check and demonstration of the applicability of our new approach also to such

删除的内容: that
删除的内容: are evenly distributed
带格式的: 字体: 10 磅
删除的内容: the
带格式的: 字体: Times New Roman
删除的内容: Such a regular distribution
删除的内容: also

gridded datasets. The ECMWF analysis fields used are based on T42L91 resolution (sampled at 2.5 °latitude × 2.5 °longitude grids, and 91 hybrid-pressure vertical levels up to about 80 km), and at the four time layers 00, 06, 12, and 18 UTC each day. This corresponds to roughly 300 km horizontal resolution that is similar to RO in the stratosphere (e.g., Kursinski et al., 1997). The 91 vertical levels correspond to about 1 km resolution in the tropopause region and gradually coarser resolution across the stratosphere, up to several kilometers in the mesosphere (Untch et al., 2006).

ECMWF data are used for cross-check in two variants. The first variant is to use the RO-collocated analysis profiles, extracted by interpolation from the analysis fields to the RO event locations, together with the OPSv5.6 RO profiles. We apply the approach in the same way to these collocated analysis profiles as to the RO profiles. We note that while the density and temperature profiles derive directly from analysis field interpolations, the bending angle profiles are obtained from forward modeling (Abelian transform from refractivity profiles) in the OPSv5.6 system.

The second variant is that we directly use the ECWMF analysis data at their regularly gridded resolution of 2.5 ° × 2.5 °, and with 4 time layers per day, which makes the averaging into coarser bins straightforward in this case and hence enables to clearly assess possible (under-)sampling biases if brought in by the limited RO events coverage, given that we intend a monitoring on a daily basis. At the same time this prepares the use of the new method with reanalysis data, such as the new European Reanalysis ERA5 (Hersbach et al., 2019, 2020; Simmons et al., 2020), foreseen in parallel to the use with RO data in future long-term application over the recent decades.

2.3 SSW detection and monitoring method

Table 1 illustrates the methodology of our SSW detection. The first step is to generate RO temperature, density, and bending angle anomaly profiles by using individual RO profiles minus collocated climatological profiles, with the latter extracted from long-term gridded RO climatology fields interpolated to RO locations as described in (1), (2), and (3) of Table 1. Temperature anomalies are calculated as absolute values, while density and bending angle anomalies are calculated as relative (percentage) values, by dividing the absolute-value anomaly profiles by the collocated climatological profiles. In order to avoid the impacts of background model on bending angles, we used non-optimized bending angle in our study. Anomalies of various atmospheric parameters have been successfully used in lots of researches for SSW detection, cloud-top altitude detection and atmospheric blocking (Hitchcock and Shepherd, 2013; Biondi et al., 2015, 2017; Brunner et al., 2016). The long-term climatology was constructed monthly using RO data of the same months over 2007 to 2017. It is based on a 2.5 °latitude × 2.5 °longitude grid. At each of the grid centers, RO profiles within 300 km of the same month over the 11 years' period are used for averaging. Sensitivity tests show that our constructed RO climatology show only small differences to climatologies calculated using ECMWF analysis data.

Based on the climatology, for our time period used as a January-February average, collocated climatological profiles can be obtained through a vertical and horizontal interpolation. Figure 2 shows RO profiles and their anomaly profiles of two exemplary RO events as indicated in Fig. 1. Left panel shows that RO profiles of event1, which locates in the most warming

area, deviate more from climatological profiles than that of event2 locating in less warming area. Anomaly profiles shown in the right panel illustrate consistent larger anomalies of event1.

The next steps are to generate five basic daily updated Thresholds Exceedance Areas (TEAs) as described in (4) – (8) of Table 1. TEA is the the geographic area wherein RO gridded mean anomalies of the day exceed predefined thresholds such as 35 K or 35 %. The first step of calculating TEA is to calculate vertical mean anomaly values of selected stratospheric altitude ranges. The vertical mean anomalies are then averaged into geographic bins on a 5 °latitude × 20 °longitude grid on a daily basis over observation area 50 – 90 °N, with grid points on latitude circles from 50 °N to 85 °N and on longitude meridians from 10 °E to 350 °E (8 × 18 grid points in total).

In order to allow more RO events coming in for a reliable statistical averaging, we use overlapping bin areas on the 5 ° × 20 ° grid as well as include time-wise, with lower weight, also the neighbor days of the given day. The latitudinal extent of the bins is set to be 10 °(+/–5 °about grid point latitude) for all latitude circles. Longitudinal bin extents $\Delta\lambda$ are determined to be 30 ° (+/–15 ° about grid point longitude) at the 50 °N grid line and then gradually expand with increasing latitude in line with meridian convergence as $\Delta\lambda_{\varphi} = \Delta\lambda_{50^{\circ}} \frac{\cos(50^{\circ})}{\cos\varphi}$, where φ denotes the grid point latitudes from 50 °N to 80 °N. At the final 85 °N latitude circle (representing the polar cap area 80 – 90 °N), we just directly average data from all longitudes. The temporal extent is set to be 3 days (+/–1 day about given day), with the data of the two neighbor days getting a weight of 0.25 only, while those of the given day are weighted by 0.5. In this way the daily sampling is indeed still meaningful, while we statistically improve the robustness of the average profiles from enabling a bigger ensemble of profiles for the weighted averaging, by taking 3-day windows. Detailed sensitivity tests showed that these selections of gridding and of spatial and temporal extents are reasonable and robust. It would allow a more reliable statistical calculation, but not blur the dynamic evolution of the SSW. Based on this averaging scheme, the number of RO profiles available per grid bin for the daily-updated averaging ranges from 60 to more than 120 profiles.

To examine various atmospheric layers, five basic TEAs are calculated, i.e., MSTA-TEA (Middle Stratosphere Temperature Anomaly TEA); LMBA-TEA, (Lower Mesosphere Bending angle Anomaly TEA); LSTA-TEA (Lower Stratosphere Temperature Anomaly TEA); USDA-TEA (middle and Upper Stratosphere Density Anomaly TEA); USTA-TEA (Upper Stratosphere Temperature Anomaly TEA). The altitude ranges for calculating these TEAs are selected according to the response altitude ranges of the three anomalies and also the utilities of the TEAs in formulating the metrics. Response altitude ranges are regarded as the altitude ranges where anomalies show distinct increases and decreases to reflect with good sensitivity the thermodynamic changes caused by an SSW event. Based on our inspections of small ensembles of individual RO anomaly profiles and also results of Sect. 3.1 on polar mean anomaly profiles, the response altitude ranges for calculating the five TEAs are carefully selected according to their utilities in measuring SSW. MSTA-TEA and LMBA-TEA are used to capture the sudden warming and are therefore calculated using temperature anomalies of 30–35 km and bending angle anomalies of 50–55 km. LSTA-TEA and USDA-TEA are used to examine the downward propagated warming and therefore they are calculated using temperature and density anomalies in lower response altitude ranges, i.e., 20–25 km for LSTA-TEA and 40–45 km for

删除的内容: 40

删除的内容: 40

删除的内容: the

带格式的: 定义网格后不调整右缩进, 段落间距段前: 0.5 行, 不调整西文与中文之间的空格, 不调整中文和数字之间的空格

删除的内容: Our

删除的内容: suggest that good

删除的内容: of temperature, density and bending angle to SSW are 20–25 km, 30–35 km, 40–45 km, and 50–55 km, respectively. Based on the chosen response altitude ranges, the variables and ranges actually used

USDA-TEA. Finally, USTA-TEA is to capture the upper stratospheric cooling in the SSW trailing phase and is calculated using temperature anomalies of 40–45 km.

As the thresholds for calculating these five TEAs, we use those defined in Table 1, (4)–(8); for example, the thresholds for MSTA are 30, 35, and 40 K as seen therein. The selection of these thresholds was mainly guided by results on the polar-mean and regional mean anomalies shown in Sections 3.1 and 3.2. We examined the temporal variations of the magnitudes of warming and cooling of the five TEAs by sensitivity checks and finally chose suitable thresholds as summarized in Table 1 for the analysis of this 2009 event. Figure 3 illustrates our selection of height ranges of anomaly profiles for calculating the five TEAs based on representative example profiles. The short vertical lines represent vertical mean values in corresponding altitude ranges. For this RO event, temperature vertical mean anomalies at the 40–45 km, 30–35 km, and 20–25 km ranges are about 25 K, 55 K, and 15 K, respectively. The density vertical mean anomaly at 40–45 km is near 40 % and the bending angle vertical mean anomaly in 50–55 km near 60 %.

Based on the five TEAs, we formulated our SSW metrics as defined in Table 1, (9)–(13), where (9)–(11) are the preferred metrics while (12)–(13) are fallback metrics for (9)–(10) requiring only temperature as variable. First is the SSW Primary-Phase metric SSW-PP-TEA (9), used to express the main and primary sudden stratospheric warming anomaly strength. It is calculated by averaging the exceedance areas MSTA-TEA>35 K and LMBA-TEA>35%. The Secondary-Phase metric SSW-SP-TEA (10) is used to express the downward propagated warming anomaly strength, and is estimated by averaging the areas LSTA-TEA>20K and USDA-TEA>30%. The Trailing-Phase metric SSW-TP-TEA (11) is expressing the trailing upper stratospheric cooling anomaly strength, and is estimated by using the area USTA-TEA<–35 K. The thresholds for formulating the metrics are selected based on the condition that the TEAs calculated for the chosen thresholds can suitably capture the main features of warming or cooling of the SSW event.

The preferred primary- and secondary-phase metrics (9) and (10) are constructed as a two-variable estimate (combining temperature and bending angle/density TEAs), since we find them more robust for characterizing the main phase of the SSW than single-variable metrics. However, users who prefer a simplified approach, or who only have stratospheric temperature profiles or fields available (within 20 to 45 km), can use the temperature-only metrics (12)–(13) instead, which do not include the averaging with the TEAs co-estimated from bending angle (9) or density (10).

Based on the three metrics, either (9)–(11) or (12)–(13) and (11), we can finally detect a SSW event and monitor the strength of the event. We introduce three SSW indicators for this purpose as defined in Table 1, (14)–(16). The first is main-phase duration, SSW-MPD, which indicates the duration of the SSW warming anomaly based on the primary- and secondary-phase metrics. This indicator is estimated by counting the number of days with either the SSW-PP-TEA or the SSW-SP-TEA being larger than a minimum exceedance area TEA_{Min}. The latter is set to the plausible value of 3 Mio. km^2 in this demonstration study (an area of ~1000 km effective radius around center location) and may become somewhat adjusted in longer-term application. The second indicator is main-phase area, SSW-MPA, which represents the mean daily threshold exceedance area during the main-phase duration. Combining these two indicators into an area-duration product yields the main-phase strength,

删除的内容:).
删除的内容: determined by careful sensitivity tests and
删除的内容: the
删除的内容: Sects
删除的内容: 60
删除的内容: 20
删除的内容: 50
删除的内容: 70
删除的内容: 40
删除的内容: 40
删除的内容: 25K
删除的内容: 40
删除的内容: 40K.
删除的内容: then

SSW-MPS, as the third and overall indicator of the severity of the SSW, enabling a classification into weak, medium, and strong events for example.

In a follow-on work using long-term RO and reanalysis datasets, these indicators will be used to detect SSW events, for example by requiring a minimum main-phase duration of 7 days or so to qualify as an SSW, and to record the strength of the events. However, the specific thresholds for our metrics and indicators for SSW detection, monitoring, and classification can only be determined after the new approach is applied to longer-term data containing multiple events.

Below we demonstrate the utility to do so, both for profile-based RO and gridded analysis data, for the Jan-Feb 2009 SSW event. In addition to demonstrating the detection and monitoring approach, we also demonstrate the parallel possibility intrinsic in our TEA-based approach to dynamically track the geographic movements of any event of interest. For this purpose we introduce the parameters Anomaly Maximum/Minimum (AM) value, and the location of these AM values, which can be used to locate the warming/cooling centers and their geographic track for the five basic TEAs. For convenience, Table 1, (17)–(18), lists and briefly explains also these auxiliary parameters.

3 Results and discussion

Section 3.1 presents temporal evolution of polar-cap mean RO anomaly profiles to have a general understanding of the characteristics of RO anomalies. Section 3.2 shows the distribution of RO gridded mean anomalies on several selected days for providing insight on the basic space-time dynamics tracked by the approach. Section 3.3 introduces our detection results of the Jan-Feb 2009 SSW demonstration event in terms of the five basic TEAs at selected thresholds and also discusses the SSW metrics of the event.

3.1 Polar-cap mean anomalies

Figure 4 shows the temporal evolution of polar cap (60 ° – 90 °N) mean temperature, density and bending angle anomaly profiles of RO data and collocated ECMWF data during the days of January and February 2009. RO temperature, density, and bending angle anomalies in their response altitude ranges show clear positive anomalies (>10 K / >10 %) from Jan 18 that quickly increase up to more than 20 K / 30 % on Jan 22-23 and then quickly decrease. Such rapid increase and decrease of positive anomalies indicate a strong and rapid warming in the middle stratosphere. The positive anomalies propagate downwards to lower altitude levels (lower stratosphere for temperature, middle stratosphere for density and bending angle) and cause longer-lasting anomalous conditions there till the end of February.

Before the sudden and rapid warming, negative anomalies are found for all the three parameters, indicating a moderate pre-cursor cooling of the stratosphere. The cooling signal is imprinted more strongly in the density and bending angle anomalies in the upper stratosphere and lower mesosphere than it is observed in temperature over the lower and middle stratosphere. After the sudden warming, negative (cooling) anomalies are again found at higher altitude levels than altitude levels showing of the sudden and rapid warming, with a particular strong imprint in upper stratosphere temperature, where its fingerprint lasts

删除的内容: settings
删除的内容: robust
删除的内容: based on the defined duration and area indicators
删除的内容: given as part of the application of
删除的内容: the long
删除的内容: 30
删除的内容: , lower stratosphere for temperature
删除的内容: the main response

over many weeks while the altitude of maximum cooling exhibits a slow downward propagation. Related to the chosen altitude layers for computing the five TEAs, we can see that they are defined so that they can well capture the SSW evolution from the initial phase to the trailing phase.

Comparing the RO profiles-based anomalies with the ECMWF analysis-based anomalies, we find that both the magnitudes and dynamical variations of the anomalies from the two datasets are generally consistent below about 45 km. The differences are found above 45 km, where RO data show larger positive density and bending angles anomalies during the sudden warming and smaller negative temperature anomalies compared to ECMWF data, from early February after the sudden warming. These increased differences are attributable to both datasets for the following reasons: (1) ECMWF data are of sparse vertical resolution and with limited constraint from assimilated data above 50 km (e.g., Untch et al., 2006; Simmons et al., 2020), degrading their accuracy; (2) RO data accuracy reaches somewhat higher in bending angle and density profiles (errors <1 % to about 50-60 km) and less high in temperature (<1 % to about 40 km); e.g., Steiner et al., 2020), so that also for these data the accuracy degrades above 45 km. In the follow-on work using long-term datasets with a range of SSW events we will analyze the different qualities of RO and (re)analysis datasets more closely, including for different RO processing and (re)analysis variants.

3.2 Spatial and temporal variations of RO anomalies

Figure 5 shows distributions of MSTA, USDA and USTA anomalies over 50 °– 90 °N on four exemplary days of Jan 15, Jan 22, Jan 29, and Feb 12, 2009, depicting the space-time dynamics of the SSW event during different phases of its evolution. Looking at MSTA results, temperature anomalies are generally negative in most of the regions on Jan 15 with values up to –40 K. Positive anomalies emerge over the northern part of Atlantic Ocean (0 °– 60 °W, 50 °– 55 °N). From that day on, positive anomalies move towards to higher latitudinal regions (can be seen from map results of other days not shown here, and from tracking of TEAs AM values discussed in Sect. 3.3 below). The magnitudes of the anomalies increase and the area of warming enlarges during the week after. This indicates an increase of the strength of the warming.

On Jan 22, positive temperature anomalies dominate the whole polar-cap region across the Atlantic sector, from over North America to over Europe. The warmest region is found centered on Greenland with anomalies exceeding 50 K. Results in this section (and in Sect. 3.3 below) indicate that Jan 22, 2009, is the warmest day of this SSW event. With the further progression of time, positive anomalies decrease, indicating a decrease of the strength of the warming. On Jan 30, smaller temperature anomalies up to 20 K are found. On Feb 12, which is two weeks after the warmest day, negative anomalies up to –20 K are found. Results of the LMBA (not shown) confirm that variations of bending angle anomalies are generally consistent with temperature anomalies, confirming the capability of RO bending angle to serve as a valuable support variable for monitoring SSWs, since this RO variable is observed accurately to better than 1 % up to about 60 km altitude (cf. Sect. 3.1).

USDA results, which are well suited to capture the downward propagated positive anomalies, show largest anomalies at the end of January. The warmest region is found from over Eastern Greenland to oceanic regions north of Russia. On Feb 12, large positive anomalies still occupy most of the polar region indicating a long-lasting warming effect caused by the SSW. The

删除的内容: 50
删除的内容: 50
删除的内容: 50
删除的内容: .
删除的内容: 16
删除的内容: 23
删除的内容: 30
删除的内容: 13
删除的内容: 16
删除的内容: 30
删除的内容: 23
删除的内容: 23
删除的内容: 13
删除的内容: 13

USTA results show positive (warming) anomalies on the initial two days illustrated. However, on Jan 29, cooling anomalies are found to occupy most of the polar region. On Feb 12, the magnitude of the cooling anomalies increases to more than –50 K and the area of strong cooling is enlarged. This indicates a strong upper stratospheric cooling, with maximum cooling centered over the Oceanic part north of Russia.

3.3 SSW detection and monitoring results

Figure 6 shows the temporal evolution of the MSTA-TEA, LMBA-TEA, LSTA-TEA, USDA-TEA, and USTA-TEA results that instructively exhibit the threshold exceedance area changes during the SSW event. The geographic tracking of maximum (positive and negative) anomaly (AM) values is also shown. MSTA-TEA and LMBA-TEA results (first two rows) are generally of similar characteristics, with positive anomalies emerging from Jan 17/18 which then quickly increase to maximum values on Jan 22/23. MSTA-TEAs are found to be largest on Jan 22, amounting for threshold exceedance areas over 30, 35 and 40 K to 13, 10, and 7 Mio. km^2, respectively. LMBA-TEA values are found to be largest on Jan 22, with areas exceeding the 30 %, 35 %, and 40 % thresholds amounting to 13, 11, and 8 Mio. km^2.

After the maximum value day, both MSTA-TEA and LMBA-TEA quickly decrease to zero. Such quick increase and decrease of the two metrics further reflect the sudden and rapid warming character of the SSW. Before the sudden warming, both TEAs show negative (cooling) anomalies as a pre-cursor signal. LMBA shows larger cooling anomalies with the TEA exceeding –35 % amounting to about 20 Mio. km^2. The negative anomalies show a tendency of increasing and reaching maximum on Jan 11 and then gradually decrease in approaching the beginning of the sudden warming. After the sudden warming, there is a phase of silence where no strong positive/negative anomalies (exceeding $\pm$30 K / %) are found. At the end of February, negative anomalies of both metrics emerge again. The right panel shows the tracking of AM values, indicating the movement of warming and cooling centers. It can be seen that the warming was centered over the east of Greenland, covering Greenland entirely and extending from Western Norway to East Greenland. During the most warmed days, the center locations of MSTA-TEA and LMBA-TEA AM values are close.

LSTA-TEA and USDA-TEA results are generally consistent in their evolution pattern as well, with most warming days found near the end of January and early February. Compared to the sharp increase and decrease of positive anomalies of MSTA-TEA and LMBA-TEA, the increase and decrease of LSTA-TEA and USDA-TEA are smoother, with maximum warming days somewhat delayed. The numbers of days showing positive (warming) anomalies are more than for MSTA-TEA and LMBA-TEA, indicating a longer-lasting warming at the lower stratospheric altitude levels. The locations of AM values of the warming anomalies are centered over Northern Russia. Negative (cooling) anomalies are found from early to middle January and are strongest over the oceanic part northeast of Russia. The USTA-TEA results, finally, show strong cooling anomalies from early February throughout the month until end of February (end of this demonstration study analysis period). From middle to end of February, the TEAs that exceed a cooling of –30, –35, and –40 K, respectively, amount to more than 15, 8, and 5 Mio. km^2. The cooling centers are found over the oceanic part north of Russia. These results are consistent to the strong upper

删除的内容: negative (cooling
删除的内容: 30
删除的内容: 13
删除的内容: increase
删除的内容: 40
删除的内容: 50
删除的内容: 18, 9
删除的内容: 4
删除的内容: 23
删除的内容: 40
删除的内容: 50
删除的内容: 18, 12
删除的内容: 5
删除的内容: 30
删除的内容: Eastern Canada.
删除的内容: rather
删除的内容: 40
删除的内容: 50
删除的内容: 3

stratospheric cooling in the SSW trailing phase found by a range of previous studies (e.g., Manney et al., 2008; Dhaka et al., 2015; Hitchcock and Shepherd, 2013).

Figure 7 depicts the overall results for our SSW metrics that we suggest to practically use for the detection and monitoring of SSW events. Geographic tracks of the metric-relevant temperature anomalies are shown as well. The first day on which the primary-phase metric SSW-PP-TEA exceeds 3 Mio. km^2 is Jan 19. From this day on, SSW-PP-TEA increases quickly up to maximum on Jan 22 and after Jan 23 then quickly decreases to be smaller than 3 Mio. km^2 on Jan 27. The secondary-phase metric SSW-SP-TEA shows a small warming peak several days before the most warming day of the primary-phase, and then decrease to minimum on Jan 24, after which it increases to maximum on Jan 31 and gradually decreases to be smaller than 3 Mio. km^2 on Feb 10. SSW-PP-TEA and SSW-SP-TEA comprise our defined main-phase, i.e., where either or both of these two metrics exceed 3 Mio. km^2. The number of days of this main-phase, our defined main-phase duration SSW-MPD, is found 22 days for this Jan-Feb 2009 demonstration event. The mean TEA over the main-phase duration, our defined main-phase area SSW-MPA, is 7.78 Mio. km^2 for this event. Multiplying duration and area yields the SSW's main-phase strength SSW-MPS, amounting to 171.2 Mio. km^2 days for this event. This clearly highlights that this SSW event extended over an area of near 2000 km effective radius around center location for more about two weeks; a major part of the polar cap north of 50 °N. In line with previous studies on this particular event, and also with our recent preliminary studies on several other events, the values of main-phase duration and also of the strength indicate that this is a very strong SSW event.

Summarizing relevant definitions, the first day of the main-phase is defined as the start day of the detected event and the end of the main-phase is defined as its final day. The center day is defined as the day with maximum TEA value of the primary metric, i.e., the Jan 22 of this demonstration event. The trailing metric SSW-TP-TEA (blue in Fig. 7), is an auxiliary metric to capture the long-lasting upper stratospheric cooling in the wake of the event. For this Jan-Feb 2009 event, the SSW-TP-TEA exceeds 3 Mio. km^2 from Feb 5, then gradually increases to a maximum of near 10 Mio. km^2 around middle February, and then gradually decreases to 8 Mio. km^2 at the end of the study period (end of February).

As introduced in Sect. 2.3, a simplified fallback of the approach is to use temperature as the only variable for the metric estimation. Hence we illustrate in Fig. 7 also the results, where the primary- and secondary-phase metrics are computed from temperature only (the trailing-phase metric is temperature-only anyway). These two simplified metrics are generally seen consistent with the preferred dual variable-based metrics, but it is visible that they appear somewhat more "volatile" and less robust in the sense that they exhibit more short-scale time variation. Follow-on work for a longer-term data record with a range of SSW events will analyze these characteristics in more detail.

The right panel shows that the main warming tracked by SSW-PPT-TEA (red) emerges from Norway and extends to Greenland and moves toward to higher latitudinal regions. The lower stratosphere warming (yellow/orange), tracked by SSW-SPT-TEA, is found emerging at the high latitudinal regions of Greenland and moving towards the northern part of Russia. The upper stratospheric cooling (blue) tracked by SSW-SPT-TEA is found mainly at the high latitudinal oceanic region north of Russia. These detection and monitoring results have been cross-tested using RO-collocated profiles from ECMWF analysis and also the regularly sampled ECWMF analysis fields as alternative data sources for these datasets. The results from both datasets (not

删除的内容: exceeding
删除的内容: 20
删除的内容: 23
删除的内容: first exceeds 3 Mio. km^2
删除的内容: and then gradually
删除的内容: 8
删除的内容: 19
删除的内容: 72
删除的内容: 146.6
删除的内容: it as a very strong
删除的内容: that
删除的内容: north of 50 °N
删除的内容: 23

separately shown) are found generally consistent for this demonstration event with the detection results using RO data. This indicates that, on an individual SSW event basis, RO observational data are of comparable utility as ECMWF (re)analysis data to monitor the event and the influence of sampling uncertainty is small. This verifies that the new approach is readily applied to both observational and (re)analysis data (and also model output data). As discussed in the introduction (Sect. 1) and along with the analysis data description (Sect. 2.2), follow-on work on long-term records next needs to show how the possible advantages in long-term stability and accuracy of the RO data play out or not in SSW detection and monitoring in comparison to reanalysis data.

To summarize, the metrics proposed in this study for monitoring the SSW events can well satisfy the conditions that Butler et al. (2015) suggest for proposing a standard definition (cf. Section 1). Firstly, our approach well captures the sudden warming of the main phase and also its downward propagation into the lower stratosphere as well as the cooling occurring after the warming phase in the upper stratosphere. Secondly, the approach can be used for both RO and other suitable profile data and likewise for reanalysis data, and can be applied for both post-processing and in real time. Finally, the new approach is using anomalies over several height layers, and TEAs over larger area, and hence the detection and monitoring results are not sensitive to details such as exact latitude or pressure level. Potential further refinements of the thresholds for our metrics will be determined from recently started work on multiple SSW events, using longer-term data over the recent decades.

4 Conclusion

In this study, we introduced a new approach to detect and monitor SSW events based on RO temperature, density, and bending angle anomaly profiles over 50 °N – 90 °N and demonstrated it for the well-known January-February 2009 event. The approach tracks the evolution by daily updates and is shown equally applicable to gridded (re)analysis data and, given the same type of gridded field structure, also to model output data.

Based on constructed anomaly profiles for the three variables temperature, density, and bending angle, we employed the concept of Threshold Exceedance Area (TEA), which is the geographic area wherein absolute or relative anomaly values exceed predefined threshold values, as the basis for formulating SSW metrics. Computing TEAs based on anomalies in selected stratospheric altitude layers and using adequate threshold values (mainly 35 K / 35 %), we formulated three SSW detection and monitoring metrics. As a simplified fallback, the metrics can be computed alternatively from profiles or fields of temperature only.

删除的内容: 40

删除的内容: 40

The primary-phase metric is to examine the initial main-phase of warming caused by SSW events. The secondary-phase metric is to examine the further main-phase of downward propagated warming effects during the SSW. The trailing-phase metric is an auxiliary metric to co-examine the upper stratospheric cooling in the wake of an SSW. Based on the two main-phase metrics, we introduced three key indicators for SSW detection and monitoring. The first is the main-phase duration, recording the number of days of SSW warming that exceed a defined minimum TEA (initially set to 3 Mio. km^2, corresponding to an area of about 1000 km effective radius around center location). The second is the average daily main-phase TEA during main-phase

duration, which is to quantify the average spatial extent of the event. The third is the area-duration product of the first two, termed main-phase strength, which expresses the overall strength and severity of the event.

For complementary space-dynamics information, the approach also enables, for the selected anomaly variables, daily tracking of the maximum anomaly values and of the related geographic center location of the event. In combination with the daily TEA estimates this quantifies also the approximate effective radius of the SSW-induced anomalies around the center location.

Applying the new approach for demonstration to the Jan-Feb 2009 SSW event, the detection and monitoring results find, where it is comparable, similar characteristics as previous studies using other approaches and datasets. We found that the SSW warming emerged from about Jan 18 and reached maximum on Jan 22 and then fading by Jan 27. In terms of our three indicators, the duration of the main-phase of this SSW was 22 days, with an average main-phase area of 7.78 Mio. km^2, yielding main-phase strength of 171.2 Mio. km^2 days. This indicates that it is a very strong SSW event, for which pronounced anomalies (>20 K/>30 %) extended over an area of near 2000 km effective radius around center location for about three weeks; a major part of the polar cap north of 60 °N. The geographic tracking of the SSW showed that it was centered over East Greenland, covering Greenland entirely and extending from Western Norway to Eastern Canada. Cross-check application of the approach using ECMWF analysis data showed results generally consistent with these results from RO data. This verifies the approach to be readily applied to both irregular profile-based observational, and to regular grid-based (re)analysis and model data.

Based on the encouraging demonstration in this study, follow-on work will apply the method to long-term RO and reanalysis datasets (RO overlapping 2006–2020 with reanalyses over 1979–2020) and assess its utility for long-term SSW monitoring. In this way, the most suitable settings to use for the duration, area, and overall strengths indicators for robust SSW detection, monitoring, and classification can be determined. In addition, we will be able to learn how the possible advantages in long-term stability and accuracy of the RO data play out or not in SSW monitoring in comparison to reanalysis data, including for different variants of RO processing and reanalysis. Overall, we expect the approach to be valuable for monitoring how SSW characteristics unfold event by event but also, and in particular, how they possibly vary under transient climate change and how they tele-connect to lower latitude regions.

Author contributions. Ying Li implemented the new method, performed the analysis, produced the figures, and wrote the initial draft of the manuscript. Gottfried Kirchengast served as primary coauthor, providing advice and guidance on all aspects of the design, analysis, figure production, and significantly contributed to writing of the manuscript. Marc Schwärz supported the setup and advancements of the OPSv5.6 analysis system and advised on data and algorithms. Florian Ladstädter supported RO climatology provision and use and advised on data and the algorithm as well as on the results interpretation. Yunbin Yuan advised on analysis and algorithm comparison. All authors commented on the final submitted manuscript.

Competing interests. The authors declare that they have no conflict of interest.

删除的内容: 17
删除的内容: 23
删除的内容: 19
删除的内容: 72
删除的内容: 146.6
删除的内容: clearly highlights
删除的内容: as
删除的内容: 40
删除的内容: 40
删除的内容: two
删除的内容: 2019
删除的内容: 2019

Acknowledgements. We acknowledge ECMWF (Reading, UK) for providing access to their analysis and forecast data. The research at APM (Wuhan, China) funded by the National key Research Program of China "Collaborative Precision Positioning Project" (No. 2016YFB0501900), and the Chinese Natural Sciences Foundation (grant no. 41874040, 41604033). At the WEGC (Graz, Austria) the work was supported by the Aeronautics and Space Agency of the Austrian Research Promotion Agency (FFG-ALR) under the Austrian Space Applications Programme (ASAP) project ATROMSAF1 (proj.no. 859771) funded by the Ministry for Transport, Innovation, and Technology (BMVIT).

References

Angerer, B., Ladstädter, F., Scherllin-Pirscher, B., Schwärz, M., and Kirchengast, G.: Quality aspects of the Wegener Center multi-satellite GPS radio occultation record OPSv5.6, Atmos. Meas. Tech., 10(12), 4845–4863, doi: 10.5194/amt-10-4845-2017, 2017.

Anthes, R. A.: Exploring Earth's atmosphere with radio occultation: contributions to weather, climate and space weather, Atmos. Meas. Tech., 4, 1077–1103, doi:10.5194/amt-4-1077-2011, 2011.

Ao, C. O., Mannucci, A. J., and Kursinski, E. R.: Improving GPS radio occultation stratospheric refractivity retrievals for climate benchmarking, Geophys. Res. Lett., 39, L12701, doi: 10.1029/2012GL051720, 2012.

Baldwin, M. P. and Dunkerton, T. J.: Stratospheric harbingers of anomalous weather regimes, Science, 294, 581–584, doi:10.1126/science.1063315.2001, 2001.

Biondi, R., Steiner, A. K., Kirchengast, G., and Rieckh, T.: Characterization of thermal structure and conditions for overshooting of tropical and extratropical cyclones with GPS radio occultation, Atmos. Chem. Phys., 15, 5181–5193, doi: 10.5194/acp-15-5181-2015, 2015.

Biondi, R., Steiner, A. K., Kirchengast, G., Brenot, H., and Rieckh, T.: Supporting the detection and monitoring of volcanic clouds: a promising new application of global navigation satellite system radio occultation, Adv. Space. Res., 60, 2707–2722 , doi: 10.1016/j.asr.2017.06.039, 2017.

Bosilovich M.G., Kennedy J., Dee D., Allan R., O'Neill A.: On the Reprocessing and Reanalysis of Observations for Climate. In: Asrar G., Hurrell J. (eds) Climate Science for Serving Society., Springer, Dordrecht, doi:10.1007/978-94-007-6692-1_3, 2013.

Brunner, L., Steiner, A.K., Scherllin-Pirscher, B., and Jury, M.W.: Exploring atmospheric blocking with GPS radio occultation observations, Atmos. Chem. Phys., 16, 4593–4604, doi: 10.5194/acp-16-4593-2016, 2016.

Butler, A.H., Seidel, D.J., Hardiman, S.C., Butchart, N., Birner, T., and Match, A.: Defining sudden stratospheric warmings, Bull.Amer. Meteor.Soc., 96, 1913–1928,doi:10.1175/BAMS-D-13-00173.1, 2015.

Butler, A.H. and Gerber, E. P.: Optimizing the definition of a sudden stratospheric warming, J. Climate, 31, 2337–2344, doi: 10.1175/JCLI-D-17-0648.1, 2018.

Charlton, A. J. and Polvani, L. M.: A new look at stratospheric sudden warmings. Part I: Climatology and modeling benchmarks, J. Climate., 20, 449–469, doi:10.1175/JCLI3996.1, 2007.

Dhaka, S. K., Kumar, V., Choudhary, R. K., Ho, S. P., Takahashi, M., and Yoden, S.: Indications of a strong dynamical coupling between the polar and tropical regions during the sudden stratospheric warming event January 2009, based on COSMIC/FORMASAT-3 satellite temperature data, Atmos. Res., 166, 60–69, doi:10.1016/j.atmosres.2015.06.008, 2015.

Eguchi, N. and Kodera, K.: Impacts of stratospheric sudden warming event on tropical clouds and moisture fields in the TTL: a case study, SOLA., 6, 137–140, doi:10.2151/sola.2010-035, 2010.

Foelsche, U., Scherllin-Pirscher, B., Ladstädter, F., Steiner, A.K., and G. Kirchengast.: Refractivity and temperature climate records from multiple radio occultation satellites consistent within 0.05%, Atmos. Meas. Tech., 4, 2007–2018, doi:10.5194/amt-4-2007-2011, 2011.

Gleisner, H. and Healy, S.B.: A simplified approach for generating GNSS radio occultation refractivity climatologies, Atmos. Meas. Tech, 6, 121–129, doi:10.5194/amt-6-121-2013, 2013.

Hajj, G. A., Kursinski, E. R., Romans, L. J., Bertiger, W. I., and Leroy, S. S.: A technical description of atmospheric sounding by GPS occultation, J. Atmos. Sol. Terr. Phys., 64, 451–469, doi:10.1016/S1364-6826(01)00114-6, 2002.

Harada, Y., Goto, A., Hasegawa, H., Fujikawa, N., Naoe, H., and Hirooka, T.: A Major stratospheric sudden warming event in January 2009, J. Atmos. Sci., 67, 2052–2069, doi:10.1175/2009JAS3320.1, 2010.

Hersbach, H., Bell, W., Berrisford, P., Horányi, A., Muñoz-Sabater, J., Nicolas, J., Radu, R., Schepers., D, Simmons, A., Soci, C., and Dee, D.: Global reanalysis: goodbye ERA-Interim, hello ERA5, ECMWF Newsl., 159, 17–24, doi:10.21957/vf291hehd7, 2019.

Hersbach, H., Bell, B., Berrisford, P., Hirahara, S., Horányi1, A., Muñoz-Sabater, J., Nicolas, J., Peubey, C., Radu, R., Schepers, D., Simmons, A., Soci, C., Abdalla, S., Abellan, X., Balsamo, G., Bechtold, P., Biavati, G., Bidlot, J., Bonavita, M., De Chiara1, G., Dahlgren, P., Dee, D., Diamantakis, M., Dragani, R., Flemming, J., Forbes, R., Fuentes, M., Geer, A., Haimberger, L., Healy, S., Hogan1,R.J., Hólm, E., Janisková, M., Keeley, S., Laloyaux, P., Lopez, P., Radnoti, G., De Rosnay, P., Rozum, I., Vamborg, F., Villaume, S., and Thépaut. J.-N.: The ERA5 Global Reanalysis, Q. J. ROY. METEOR. SOC. Quarterly., doi: 10.1002/qj.3803, 2020.

Hitchcock, P. and Shepherd, T. G.: Zonal-mean dynamics of extended recoveries from stratospheric sudden warmings, J. Atmos. Sci., 70, 688–707, doi:10.1175/JAS-D-12-0111.1, 2013.

Ho, S.-P., Hunt, D., Steiner, A. K., Mannucci, A. J., Kirchengast, G., Gleisner, H., Heise, S., von Engeln, A., Marquardt, C., Sokolovskiy, S., Schreiner, W., Scherllin-Pirscher, B., Ao, C., Wickert, J., Syndergaard, S., Lauritsen, K., Leroy, S., Kursinski,E. R., Kuo, Y.-H., Foelsche, U., Schmidt, T., and Gorbunov, M.: Reproducibility of GPS radio occultation data for climate monitoring: Profile-to-profile inter-comparison of CHAMP climate records 2002 to 2008 from six data centers, J. Geophys. Res., 117, D18111, doi: 10.1029/2012JD017665, 2012.

Klingler, R.: Observing Sudden Stratospheric Warmings with Radio Occultation Data, with Focus on the Event 2009, MSc thesis, University of Graz, Graz, 2014.

Kodera, K., Eguchi, N., Lee, J.N., Kuroda, Y., and Yukimoto, S.: Sudden changes in the tropical stratospheric and tropospheric circulation during January 2009, J. Meteorol. Soc. Jpn., 89, 283–290, doi:10.2151/jmsj.2011-308, 2011.

Kohma, M. and K. Sato.: Variability of upper tropospheric clouds in the polar region during stratospheric sudden warmings, J. Geophys. Res. Atmos., 119, 10100–10113, doi:10.1002/2014JD021746, 2014.

删除的内容: in review, 2020.

Kursinski, E. R., Hajj, G. A., Schofield, J. T., Linfield, R. P., and Hardy, K. R.: Observing Earth's atmosphere with radio occultation measurements using the Global Positioning System, J. Geophys.Res., 102, 23429–23465, doi:10.1029/97JD01569, 1997.

Labitzke, K. and Kunze, M.: On the remarkable Arctic winter in 2008/2009, J. Geophys. Res. Atmos, 114, D00I02, doi: 10.1029/2009JD012273, 2009.

Ladstädter, F., Steiner, A. K., Schwärz, M., and Kirchengast, G.: Climate intercomparison of GPS radio occultation, RS90/92 radiosondes and GRUAN from 2002 to 2013, Atmos. Meas. Tech., 8, 4, 1819–1834, doi:10.5194/amt-8-1819-2015, 2015.

Limpasuvan, V., Thompson, D. W. J., and Hartmann, D. L.: The life cycle of the northern hemisphere sudden stratospheric warmings, J. Climate., 17, 2584–2596, doi:10.1175/1520-0442(2004)017<2584:TLCOTN>2.0.CO;2,2004.

Lin, J. T., Lin, C.H., Chang, L.C., Huang, H.H., Liu, J.Y., Chen, A. B., Chen, C.H., and Liu, C.H.: Observational evidence of ionospheric migrating tide modification during the 2009 stratospheric sudden warming, Geophys. Res. Lett., 39, L02101, doi:10.1029/2011GL050248, 2012.

Luntama, J.-P., Kirchengast, G., Borsche, M., Foelsche, U., Steiner, A., Healy, S., von Engeln, A., O'Clerigh, E., and Marquardt, C.: Prospects of the EPS GRAS mission for operational atmospheric applications, B. Am. Meteorol. Soc., 89, 1863–1875, doi: 10.1175/2008BAMS2399.1, 2008.

Manney, G.L., Krüger, K., Pawson, S., Minschwaner, K., Schwartz, M.J., Daffer, W.H., Livesey, N.J., Mlynczak, M.G., Remsberg, E.E., Russell III, J.M., and Waters, J.W.: The evolution of the stratopause during the 2006 major warming: satellite data and assimilated meteorological analyses, J. Geophys. Res., 113, D11115, doi: 10.1029/2007JD009097, 2008.

Manney, G.L., Schwartz, M.J., Kruger, K., Santee, M.L., Pawson, S., Lee, J.N., Daffer, W.H., Fuller, R.A., and Livesey, N.J.: Auramicrowave limb sounder observations of dynamics and transport during the record-breaking 2009 Arctic stratospheric major warming, Geophys. Res. Lett., 36, L12815, doi: 10.1029/2009GL038586, 2009.

McInturff, R. M., Ed.: Stratospheric warmings: Synoptic, dynamic and general-circulation aspects, NASA Reference Publ., NASA-RP-1017, 174, 1978.

Mitchell, D. M., Charltonperez, A.J., and Gray, L. J.: Characterizing the variability and extremes of the stratospheric polar vortices using 2D moment analysis, J. Atmos. Sci., 68, 1194–1213, doi:10.1175/2010JAS3555.1, 2011.

Newman et al.: The Major Stratospheric Sudden Warming of February 2018, Thursday, 21 March 2019, Vienna, Aerosol and Environmental Physics Group, Seminar talk, 2018.

Parker, W. S.: Reanalyses and observations: What's the difference? Bull. Amer. Meteor. Soc., 97, 1565–1572, doi: 10.1175/BAMS-D-14-00226.1, 2016.

Sathishkumar, S. and Sridharan., S.: Observations of 2–4 day inertia-gravity waves from the equatorial troposphere to the F region during the sudden stratospheric warming event of 2009, J. Geophys. Res., 116, A12320, doi:10.1029/2011JA017096, 2011.

Scherllin-Pirscher, B., Kirchengast, G., Steiner, A. K., Kuo, Y.-H., and Foelsche, U.: Quantifying uncertainty in climatological fields from GPS radio occultation: an empirical-analytical error model, Atmos. Meas. Tech., 4, 2019–2034, doi:10.5194/amt-4-2019-2011, 2011a.

Scherllin-Pirscher, B., Steiner, A. K., Kirchengast, G., Kuo, Y.-H., and Foelsche, U.: Empirical analysis and modelling of errors of atmospheric profiles from GPS radio occultation, Atmos. Meas. Tech., 4, 1875–1890, doi:10.5194/amt-4-1875-2011, 2011b.

Scherllin-Pirscher, B., Syndergaard, S., Foelsche, U. and Lauritsen, K. B.: Generation of a bending angle radio occultation climatology (BAROCLIM) and its use in radio occultation retrievals, Atmos. Meas. Tech., 8, 109—124, doi:10.5194/amt-8-109-2015, 2015.

Scherllin-Pirscher, B., Steiner, A. K., Kirchengast, G.,Schwaerz, M., and Leroy, S. S.: The power of vertical geolocation of atmospheric profiles from GNSS radio occultation, J. Geophys. Res.-Atmos., 122, 1595–1616, doi:10.1002/2016JD025902, 2017.

Schwaerz, M., Kirchengast, G., Scherllin-Pirscher, B., Schwarz, J., Ladstädter, F., and Angerer, B.: Multi-Mission Validation by Satellite Radio Occultation – Extension Project, Final report for ESA/ESRIn No. 01/2016, WEGC, University of Graz, Graz, Austria, 2016.

Schreiner, W., Rocken, C., Sokolovskiy, S., Syndergaard, S. and Hunt, D.: Estimates of the precision of GPS radio occultations from the COSMIC/FORMOSAT-3 mission, Geophys. Res. Lett., 34, L04808, doi:10.1029/2006GL027557, 2007.

Seviour, W. J. M., Mitchell, D. M., and Gray, L.J.: A practical method to identify displaced and split stratospheric polar vortex events, Geophys. Res. Lett., 40, 5268–5273, doi:10.1002/grl.50927, 2013.

Simmons, A., Soci, C., Nicolas, J., Bell, B., Berrisford, P., Dragani, R., Flemming, J., Haimberger1, L., Healy, S., Hersbach, H., Horányi, A., Inness, A., Muñoz-Sabater, J Radu, R., and Schepers, D.: Global stratospheric temperature bias and other stratospheric aspects of ERA5 and ERA5.1, ECMWF Tech., Memo., No. 859, doi:10.21957/rcxqfmg0, 2020.

Siskind, D. E., Eckermann, S.D., Coy, L., Mccormack, J. P., and Randall, C.E.: On recent interannual variability of the Arctic winter mesosphere: Implications for tracer descent, Geophys. Res. Lett., 34, L09806, doi:10.1029/2007GL029293, 2007.

Steiner, A. K., Hunt, D., Ho, S.-P., Kirchengast, G., Mannucci, A. J., Scherllin-Pirscher, B., Gleisner, H., von Engeln, A., Schmidt, T., Ao, C., Leroy, S. S., Kursinski, E. R., Foelsche, U., Gorbunov, M., Heise, S., Kuo, Y.-H., Lauritsen, K. B., Marquardt, C., Rocken, C., Schreiner, W., Sokolovskiy, S., Syndergaard, S., and Wickert, J.: Quantification of structural uncertainty in climate data records from GPS radio occultation, Atmos. Chem. Phys., 13, 1469–1484, doi:10.5194/acp-13-1469-2013, 2013.

Steiner, A.K., Kirchengast，G., Foelsche, U., Kornblueh, L., Manzini, E., and Bengtsson, L.: GNSS occultation sounding for climate monitoring, Phys. Chem. Earth (A)., 26, 113-124, doi: 10.1016/S1464-1895(01)00034-5, 2001.

Steiner, A. K., Lackner, B. C., Ladstädter, F., Scherllin-Pirscher, B., Foelsche, U., and Kirchengast, G.: GPS radio occultation for climate monitoring and change detection, Radio Sci., 46, RS0D24, doi:10.1029/2010RS004614, 2011.

Steiner, A. K., Ladstädter, F., Ao, C. O., Gleisner, H., Ho, S.-P., Hunt, D., Schmidt, T., Foelsche, U., Kirchengast, G., Kuo, Y.-H., Lauritsen, K. B., Mannucci, A. J., Nielsen, J. K., Schreiner, W., Schwärz, M., Sokolovskiy, S., Syndergaard, S., and Wickert, J.: Consistency and structural uncertainty of multi-mission GPS radio occultation records, Atmos. Meas. Tech., doi:10.5194/amt-2019-358, 2019.

Sun, Y., Bai, W., Liu, C., Liu, Y., Du, Q., Wang, X., Yang, G., Liao, M., Yang, Z., Zhang, X., Meng, X., Zhao, D., Xia, J., Cai, Y., and Kirchengast, G.: The FengYun-3C radio occultation sounder GNOS: a review of the mission and its early results and science applications, Atmos. Meas. Tech., 11, 5797–5811, doi:10.5194/amt-11-5797-2018, 2018.

Taguchi, M., Latitudinal Extension of Cooling and Upwelling Signals associated with Stratospheric Sudden Warmings, Journal of the Meteorological Society of Japan, 89, 5, 571–580, 2011, doi:10.2151/jmsj.2011-511, 2011.

删除的内容: in press, 2020

Thompson, D. W. J., Baldwin, M. P., and Wallace, J. M.: Stratospheric connection to northern hemisphere wintertime weather: implications for prediction, J. Climate, 15(12), 1421–1428, doi:10.1175/1520-0442(2002)015<1421:SCTNHW>2.0.CO;2, 2002.

Untch, A., Miller, M., Hortal, M., Buizza, R., and Janssen, P.: Towards a global meso-scale model: The high-resolution system T799L91 and T399L62 EPS, ECMWF Newsl., 108, 6–13, 2006.

Wang, L. and Alexander, M. J.: Gravity wave activity during stratospheric sudden warmings in the 2007–2008 Northern Hemisphere winter, J. Geophys. Res. Atmos., 114, D18108, doi:10.1029/2009JD011867,2009.

Yoshida, K. and Yamazaki, K.: Tropical cooling in the case of stratospheric sudden warming in January 2009: focus on the tropical tropopause layer, Atmos. Chem. Phys., 11, 6325–6336, doi:10.5194/acp-11-6325-2011, 2011.

Yue, X., Schreiner, W.S., Lei, J., Rocken, C., Hunt, D.C., Kuo, Y.-H. and Wan, W.: Global ionospheric response observed by COSMIC satellites during the January 2009 stratospheric sudden warming event, J. Geophys. Res., 115, A00G09, doi: 10.1029/2010JA015466, 2010.

Wickert, J., Reigber, C., Beyerle, G., König, R., Marquardt, C., Schmidt, T., Grundwaldt, L., Galas, R., Meehan, T. K., Melbourne, W. G., and Hocke, K.: Atmosphere sounding by GPS radio occultation: First results from CHAMP, Geophys. Res. Lett., 28, 32633266, doi:10.1029/2001GL013117, 2001.

Wickert, J., Beyerle, G., König, R., Heise, S., Grunwaldt, L., Michalak, G., Reigber, Ch., and Schmidt, T.: GPS radio occultation with CHAMP and GRACE: A first look at a new and promising satellite configuration for global atmospheric sounding, Ann. Geophys., 23, 653–658,doi:10.5194/angeo-23-653-2005, 2005.

Table 1. Basic parameters and methodology of the new SSW monitoring approach (all parameters (4)–(18) updated daily).

Parameter	Equation/Definition	Explanation/Description
(1) Temperature anomaly profile $T_{Anomaly}$	$T_{Anomaly} = T_{RO} - T_{ROCli}$	T_{RO}: RO temperature profile ; T_{ROCli}: collocated climatological profile
(2) Density anomaly profile $\rho_{Anomaly}$	$\rho_{Anomaly} = (\rho_{RO} - \rho_{ROCli}) / \rho_{ROCli} \times 100\%$	ρ_{RO}: RO density profile; ρ_{ROCli}: collocated climatological profile
(3) Bending angle anomaly profile $\alpha_{Anomaly}$	$\alpha_{Anomaly} = (\alpha_{RO} - \alpha_{ROCli}) / \alpha_{ROCli} \times 100\%$	α_{RO}: RO bending angle profile; α_{ROCli}: collocated climatological profile
(4) Middle Stratosphere Temperature Anomaly Threshold Exceedance Area: **MSTA-TEA**	Altitude range: 30–35 km Thresholds selected: +40 K, +35 K, +30 K; –30 K, –35 K, –40 K	Extract from individual anomaly profiles in selected stratosphere and stratopause region altitude layers (e.g., 30–35 km for MSTA-TEA) to estimate a vertical mean anomaly value for all RO events. The vertical mean anomalies are then averaged into a suitable space-time-binned grid over 50–90 °N (5 ° latitude × 20 °longitude grid). The geographic areas wherein temperature, density and bending angle anomalies exceed predefined thresholds such as 35 K or 30 % are calculated and denoted as Threshold Exceedance Areas (TEAs).
(5) Lower Mesosphere Bending angle Anomaly Threshold Exceedance Area: **LMBA-TEA**	Altitude range:50–55 km Thresholds selected: +40 %, +35 %, +30 %; –30 %, –35 %, –40%	
(6) Lower Stratosphere Temperature Anomaly Threshold Exceedance Area: **LSTA-TEA**	Altitude range: 20–25 km Thresholds selected: 30 K, 25 K, 20 K;-20 K, -25 K, -30 K	
(7) Upper Stratosphere Density Anomaly Threshold Exceedance Area: **USDA-TEA**	Altitude range: 40–45 km Thresholds selected: 40%,35 %, 30 %; -30 %, -35 %, -40 %	
(8) Upper Stratosphere Temperature Anomaly Threshold Exceedance Area: **USTA-TEA**	Altitude range: 40–45 km Thresholds selected: +40 K, +35 K, +30 K; –30 K, –35 K, –40 K	
(9) Primary-phase metric: **SSW-PP-TEA**	SSW-PP-TEA [km^2] = Avg(MSTA-TEA>35 K, LMBA-TEA>35%)	Expresses the main and primary stratospheric warming anomaly strength
(10) Secondary-phase metric: **SSW-SP-TEA**	SSW-SP-TEA [km^2] = Avg(LSTA-TEA>20K, USDA-TEA>30%)	Expresses the secondary downward propagated warming anomaly strength
(11) Trailing-phase metric: **SSW-TP-TEA**	SSW-TP-TEA [km^2] = Abs(USTA-TEA<–35K)	Expresses the trailing upper stratosphere cooling anomaly strength
(12) Primary-phase T-only metric: **SSW-PPT-TEA**	SSW-PPT-TEA [km^2] = (MSTA-TEA>35K)	Complementary primary metric using only temperature information
(13) Secondary-phase T-only metric: **SSW-SPT-TEA**	SSW-SPT-TEA [km^2] = (LSTA-TEA>20K)	Complementary secondary metric using only temperature information
(14) Main-phase duration: **SSW-MPD**	SSW-MPD [days] (definition see right column)	Number of days with SSW-PP-TEA or SSW-SP-TEA > TEA_{Min} (3 Mio. km^2)
(15) Main-phase area: **SSW-MPA**	SSW-MPA [Mio. km^2] (definition see right column)	Mean daily Max(SSW-PP-TEA, SSW-SP-TEA) during all SSW-MPD days
(16) Main-phase strength: **SSW-MPS**	SSW-MPS [Mio. km^2 days] = (SSW-MPA x SSW-MPD)	Overall strength, the larger this area-duration product, the stronger the event
(17) Anomaly Maximum (AM) values	ΔT_{Max} [K], $\Delta\alpha_{Max}$ [%], $\Delta\rho_{Max}$ [%]	Maximum (positive/negative) anomaly values of all grid cells over 50 °N-90 °N
(18) Geographic location (Lat, Lon) of AM values	φ^{AM} [°N], λ^{AM} [°E]	Generate a contour that is 2 K / 2 % smaller/larger than the positive/negative AM value; the center of the contour is then used as location of the AM value

删除的内容: $T_{Anomaly} = T_{RO} - T_{ROCli}$

域代码已更改

删除的内容: $\rho_{Anomaly} = (\rho_{RO} - \rho_{ROCli}) / \rho_{ROCli} \times 100\%$

域代码已更改

删除的内容: $\alpha_{Anomaly} = (\alpha_{RO} - \alpha_{ROCli}) / \alpha_{ROCli} \times 100\%$

域代码已更改

删除的内容: +50 K,

删除的内容: , –50 K

删除的内容: +50 %,

删除的内容: %, . –50

删除的内容: 50 %,

删除的内容: %, -50

删除的内容: 40

删除的内容: 40

删除的内容: +50 K,

删除的内容: , –50 K

删除的内容: 40K

删除的内容: 40

删除的内容: 25K

删除的内容: 40

删除的内容: 40K

删除的内容: 40K

删除的内容: 25K

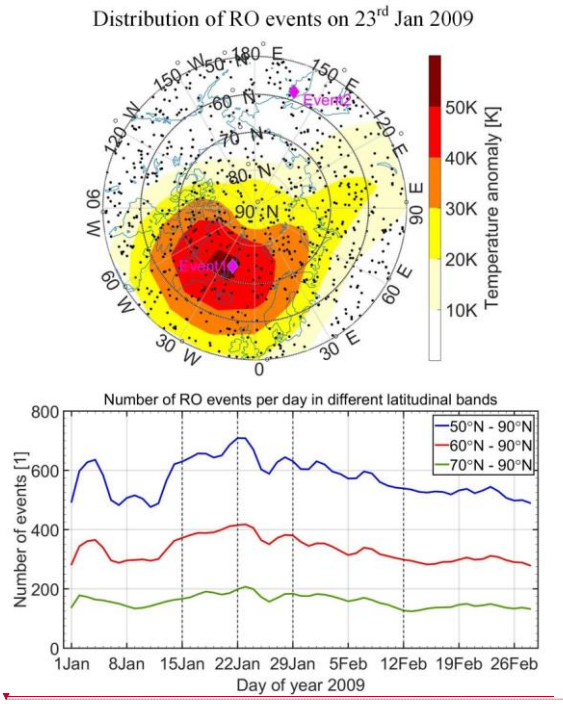

删除的内容：

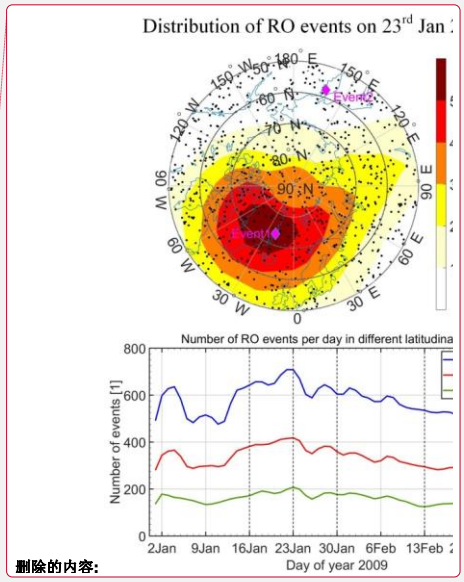

Figure 1. Illustrative distribution of RO event locations on 23 Jan 2009 (black dots), overplotted on the middle-stratosphere temperature anomaly of the day (upper panel), and number of RO events per day in the latitudinal bands of 50 – 90 °N (blue), 60 – 90 °N (red), and 70 – 90 °N (red), during January and February of 2009 (lower panel). In the upper panel, "Event1" represents an RO event with a large temperature anomaly, and "Event2" one with small anomaly (diamond symbols), as used in the subsequent Figs. 2 and 3.

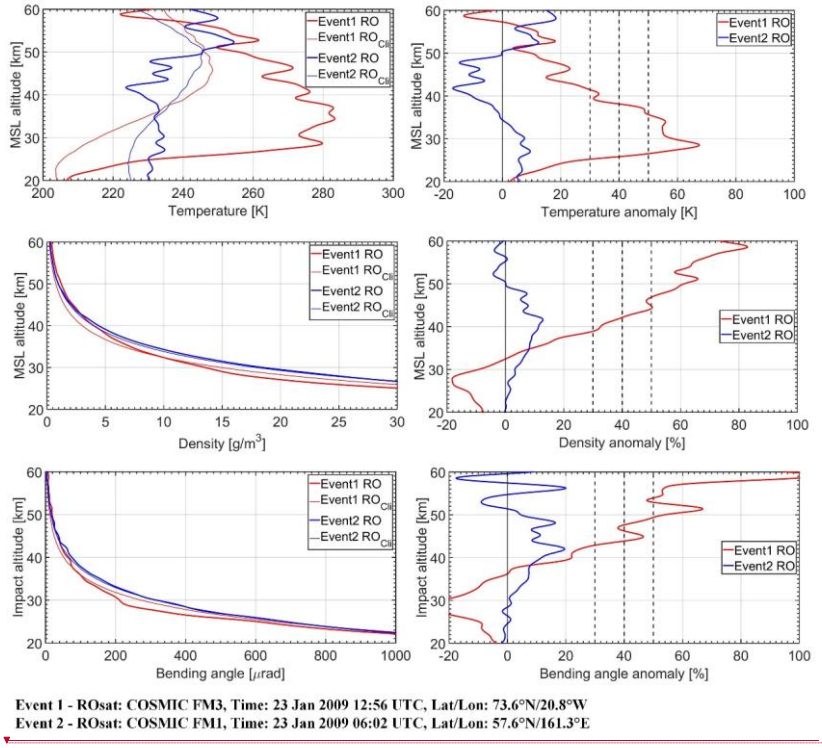

Figure 2. Event1 and Event2 temperature (top), density (middle), and bending angle (bottom) profiles from RO and their collocated climatological profiles RO_{Cli} (left column), together with the corresponding anomaly profiles (right column), the latter computed according to Table 1, (1) – (3).

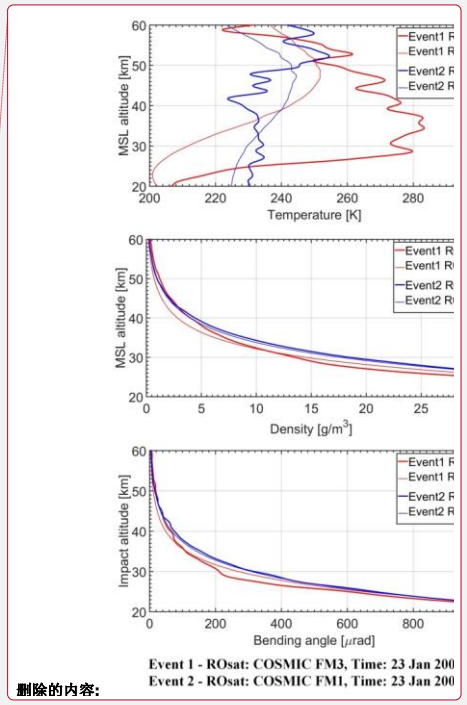

删除的内容:

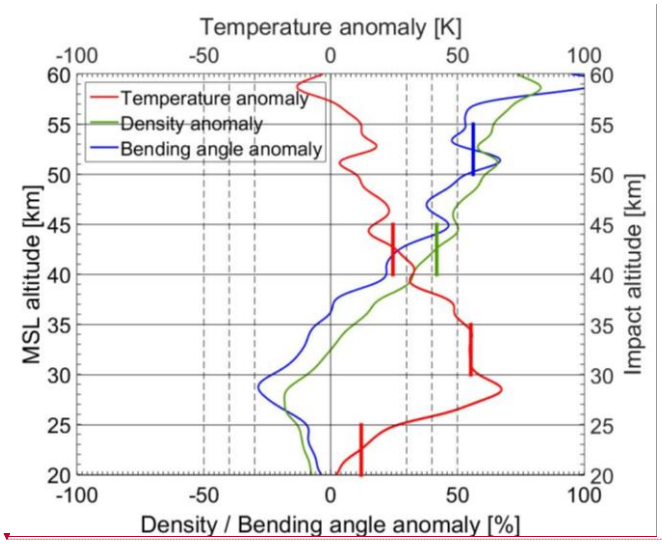

删除的内容:

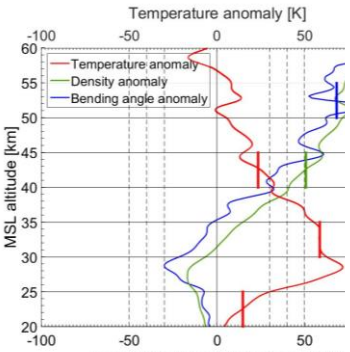

Figure 3. Temperature (blue), density (green) and bending angle (red) anomaly profiles of Event1 (same as in Figs. 1 and 2), with the horizontal gray lines delineating the altitude layers chosen for calculating the five basic TEAs (Table 1, (4) – (8)) and the colored vertical thick lines indicating the vertical mean anomaly values in corresponding altitude layers.

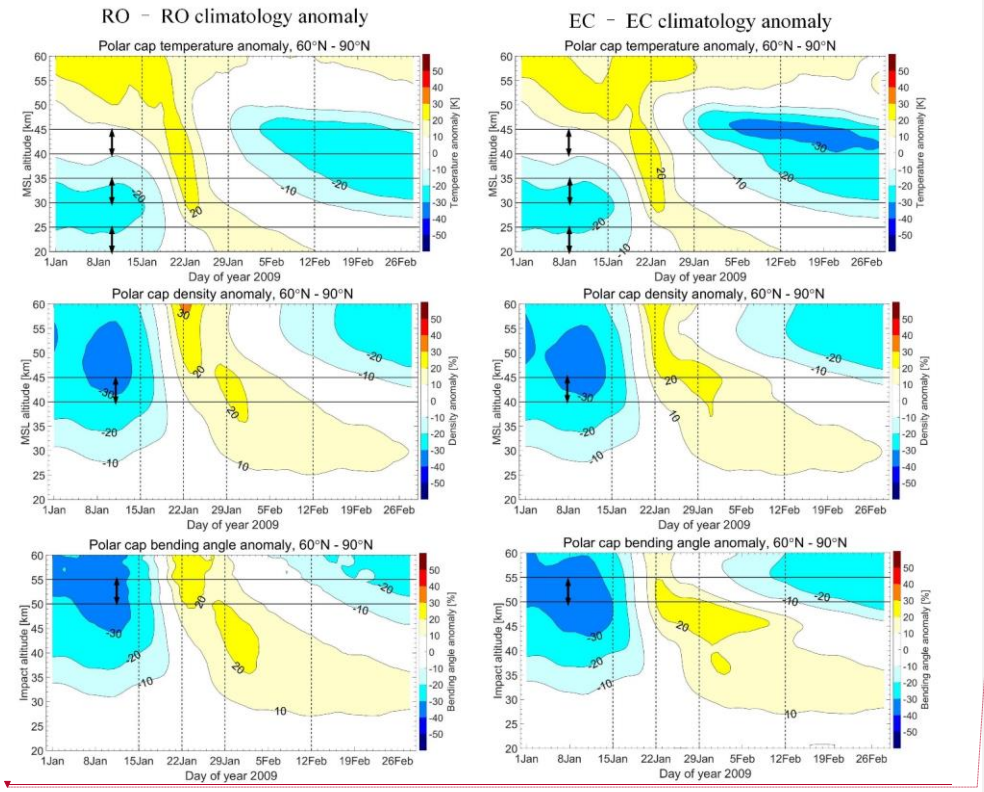

删除的内容:

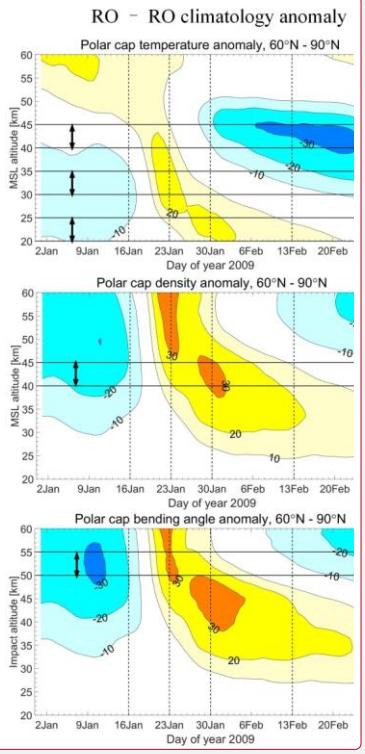

Figure 4. Temporal evolution of polar-cap (60 °– 90 °N) mean temperature (top), density (middle), and bending angle (bottom) anomaly profiles from RO (left column), complemented by the corresponding anomalies from the ECMWF analysis data (right column). The vertical dashed lines indicate four days selected for showing anomaly distributions in Fig. 5 and the horizontal lines in the panels delineate those altitude layers chosen for the respective variables to help compute the TEA metrics as presented in Fig. 3.

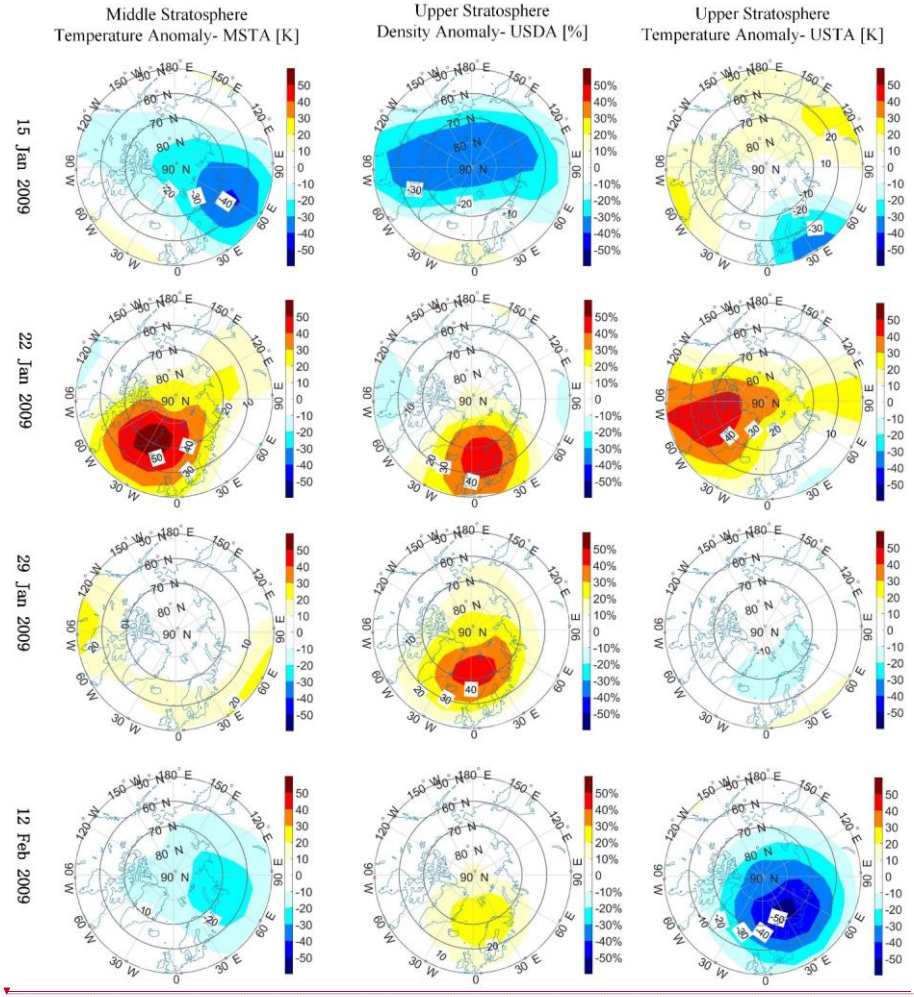

Figure 5. Middle Stratosphere Temperature Anomaly (MSTA, left column), Upper Stratosphere Density Anomaly (USDA, middle column) and Upper Stratosphere Temperature Anomaly (USTA, right column) on the four exemplary days of Jan 15, Jan 22, Jan 29, and Feb 12, 2009, illustrating the space-time dynamics of the SSW event in these three anomaly quantities.

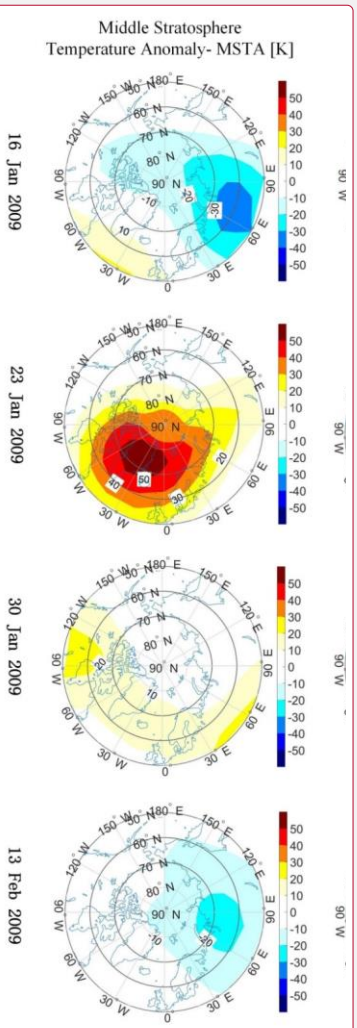

删除的内容:

删除的内容: 16…5, Jan 23…2, Jan 30…9, and Feb 13

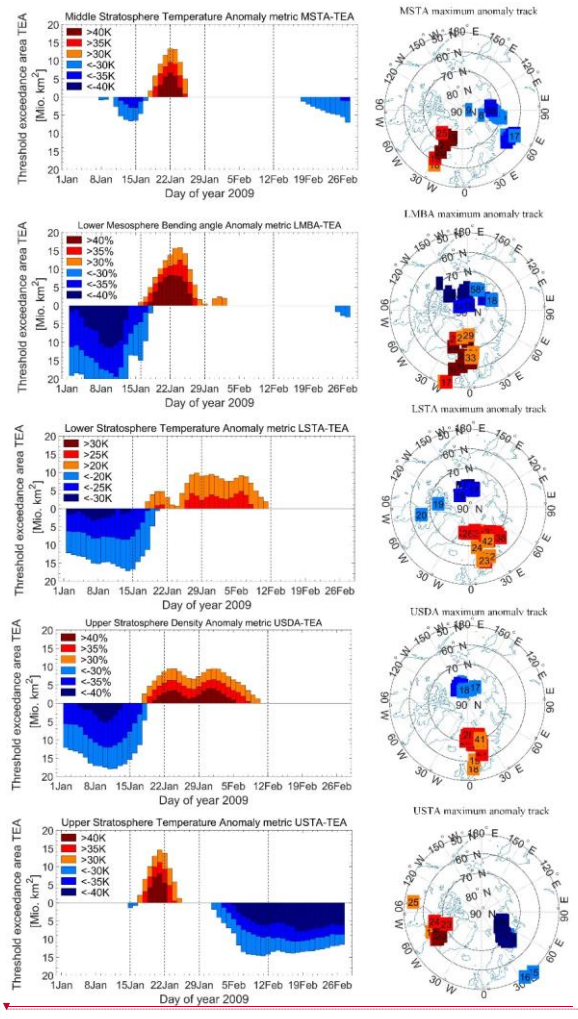

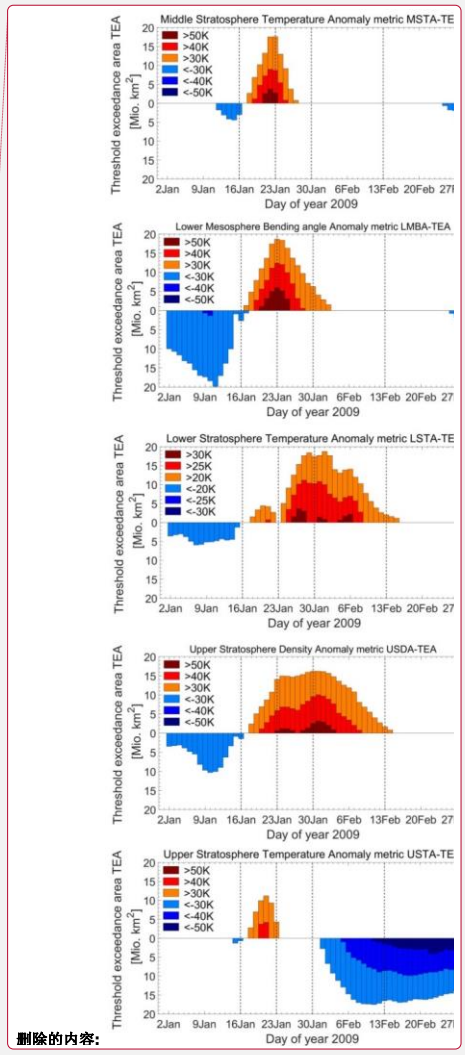

删除的内容:

Figure 6. Time evolution of the daily MSTA, LMBA, LSTA, USDA, and USTA (from top to bottom) Threshold Exceedance Areas (TEAs) during the SSW event, using thresholds according to Table 1, (4)–(8) (left column). For complementary space-dynamics information, geographic tracks and magnitude classes (color scheme of left panels, numbering by day-of-year) of maximum positive/negative anomaly values are shown (right column).

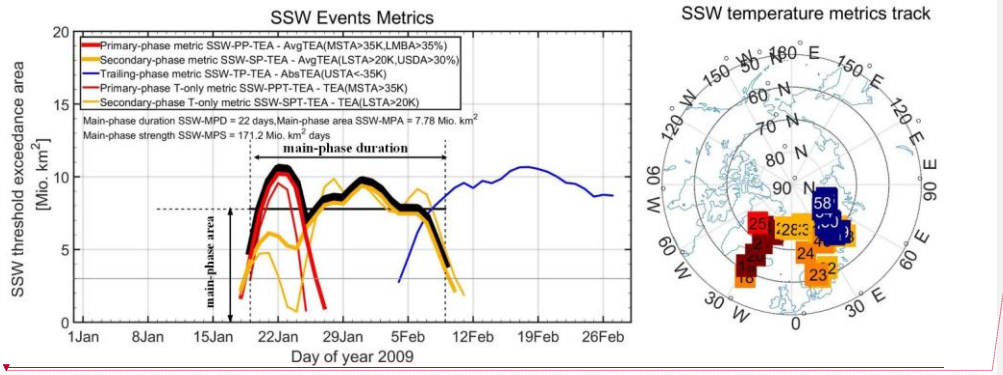

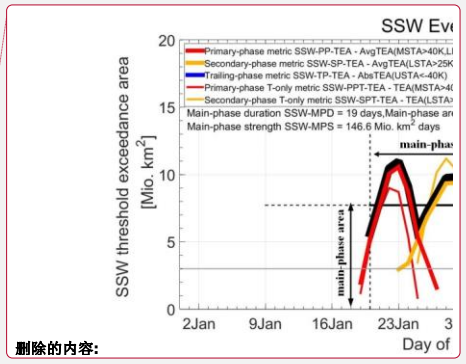

删除的内容:

Figure 7. Time evolution of the daily primary-phase (heavy red), secondary-phase (heavy yellow), trailing-phase (heavy blue), primary-phase temperature-only (light red), and secondary-phase temperature-only (light yellow) metrics, respectively (left panel), shown for daily TEAs exceeding 1 Mio. km^2. The main-phase metrics envelope for computing the main-phase area and duration (heavy black) and the related area, duration, and strength indicator results are depicted as well (the numeric results in legend) and the TEA_{Min} threshold of 3 Mio. km^2 is indicated as gray horizontal line. For complementary space-dynamics information, the geographic tracks and magnitude classes of the three metric-relevant temperature anomalies (MSTA red, LSTA yellow, USTA blue) are also shown (right; style as in right panels of Fig. 6).